Changes in macromolecular organization in collagen assemblies during secretion in the nidamental gland and formation of the egg capsule wall in the dogfish *Scyliorhinus canicula*

DAVID P. KNIGHT[1], DIAN FENG[1], MURRAY STEWART[2] AND ELIZABETH KING[1]

[1]*Department of Biological Science, King Alfred's College, Sparkford Road, Winchester SO22 4NR, U.K.*
[2]*Medical Research Council Laboratory of Molecular Biology, Cambridge CB2 2QH, U.K.*

SUMMARY

The thickest layer (L_2) of the egg capsule wall of the dogfish, *Scyliorhinus canicula*, is constructed largely from highly ordered collagen fibrils (Knight & Hunt 1976). This collagen is stored and secreted by the nidamental gland and passes through an extraordinary series of ordered phases, many of which have well defined liquid crystalline structure. We have examined the changes in macromolecular packing of the collagen as it moves from the cisternae of the endoplasmic reticulum to secretory granules, is secreted and then formed into the egg capsule wall. Within the endoplasmic reticulum cisternae the collagen appears anisotropic but becomes assembled into a smectic A or lamellar phase in the Golgi cisternae. This phase persists in early secretory granules, where it is found in conjunction with a micellar phase. As these granules mature, the collagen passes through a cholesteric mesophase before adopting a columnar hexagonal arrangement. On merocrine secretion the granules' contents revert rapidly to the smectic A-lamellar and micellar phases. As it passes along the nidamental gland tubules, the collagen is first converted into a second distinct micellar phase before assembling into the final fibrils that constitute the egg capsule. These phase transitions give powerful insights into the way in which the macromolecular arrangement of collagen molecules can be modulated and are discussed in the context of a range of other related structural transitions in collagens.

1. INTRODUCTION

The egg capsule of the dogfish, *Scyliorhinus canicula*, is constructed largely from collagen-containing fibrils with a unique crystalline arrangement (Rusaouën *et al.* 1976; Knight & Hunt 1976, 1986). The collagen in these fibrils is secreted in a clearly defined zone (the D-zone) which forms the bulk of the nidamental gland (Rusaouën-Innocent 1990*a*,*b*; Feng & Knight 1992). Rusaouën (1978) has described the ultrastructure of the D-zone secretory cells. The collagen appears to be stored in large numbers of membrane-bound granules in these cells (Rusaouën-Innocent 1990*b*). We (Knight & Feng 1992) have recently described the pathway by which collagen is secreted and incorporated into the egg capsule and proposed a mechanism by which the orientation of the collagen-containing fibrils is defined.

Here we describe in detail the different defined ways in which collagen molecules assemble with one another as they pass through this secretion pathway. This pathway contains an extraordinarily varied number of collagen macromolecular assemblies and, because different temporal forms are separated spatially, this system has unique advantages for studying the mechanism of collagen assembly and the modulation of different collagen macromolecular aggregates.

2. MATERIALS AND METHODS

(*a*) *Material*

Female dogfish, *Scyliorhinus canicula*, were obtained by line fishing. Ripe females can be recognized by their girth and by the pale orange coloration of the skin immediately surrounding the vent.

(*b*) *Preparation of material for microscopy*

Nidamental glands were taken from fish that were in the act of secreting a capsule or contained fully formed capsules within the oviduct. They were prepared for transmission electron microscopy (TEM), scanning electron microscopy (SEM) and cryostat sectioning for bright field and polarizing microscopy as described elsewhere (Feng & Knight 1992; Knight & Feng 1992). Except where stated, material was fixed at 20°C by perfusion in a solution containing 1% glutaraldehyde,

Phil. Trans. R. Soc. Lond. B (1993) **341,** 419–436
Printed in Great Britain

3% paraformaldehyde, 0.1 M sodium cacodylate/HCl buffer (pH 7.4), 0.45 M sodium chloride and 2 mM calcium chloride. After post-fixation in buffered osmium tetroxide solution and *en bloc* staining with uranyl acetate, material was embedded in Spurr's resin. Tissues were routinely stained *en bloc* with aqueous uranyl acetate. Ultrathin sections were stained with saturated uranyl acetate in 50% ethanol followed by 2% aqueous phosphotungstic acid at pH 6.5 followed by Reynold's lead citrate. Some ultrathin sections were stained with uranyl acetate and lead citrate without the phosphotungstic acid step. The micrographs presented here are taken from sections of the most anterior three to four rows of D tubules. The secretory granules in the more posterior D tubules are essentially similar but contain globules of an additional dense component which complicated analysis.

Measurements of periodicities were made directly from prints on regions showing sharp banding patterns or lattices. Negatively stained bovine catalase crystals were used to calibrate the TEM magnification. Standard deviations are reported ($n = > 15$).

(*c*) *Computer image processing*

Optical diffraction was used to select well-ordered areas in which focus and astigmatism correction were optimal. These areas were digitized on a square raster and processed using the usual Fourier-based methods reviewed by Stewart (1986, 1988). Briefly, suitable areas were windowed off and, after reducing their average edge density to zero and apodization, were embedded in arrays of 1024 × 1024 zeros and Fourier transforms computed. The crystalline lattice points were identified in the Fourier transform and masked off. The remainder of the transform was then set to zero and a filtered image computed by Fourier inversion.

(*d*) *Biochemistry*

The solubility of the collagen within nidamental gland D-zone cells was demonstrated by briefly extracting unfixed cryostat sections with 0.1 M acetic acid at 10°C before fixation with 4% formaldehyde in 0.1 M phosphate buffer at pH 7.4 and subsequent staining with Mallory's aniline blue (Gray 1973). Solubility of the collagen was confirmed by homogenizing nidamental glands in cold 0.1 M acetic acid containing all the inhibitors used by Angermann & Barrach (1979) together with those used by Niemalä *et al.*(1985). Collagen was precipitated by ammonium sulphate (20% saturation), resuspended in 0.1 M acetic acid and applied to a DEAE-Sephadex column (720 mm × 30 mm) previously equilibrated with 0.1 M acetic acid. The column was eluted with a 1 litre linear 0–1 M salt gradient in 0.1 M acetic acid. A Sircol collagen assay kit (Qubis Ltd, Belfast) was used to follow collagen purification (Woessner 1976). After freeze drying, fractions were run on precast (10%) or gradient (7.5–15%) sodium dodecyl sulphate (SDS) polyacrylamide mini gels (Biorad Ltd) at pH 8.6 and stained with Coomassie blue. SDS polyacrylamide electrophoresis was also applied to extracts of the most recently secreted part of the white egg capsule, prepared by heating scrapings from layer L_2 at 100°C for five minutes in a small volume of sample buffer containing SDS with or without mercaptoethanol.

The pH of the recently formed egg capsule wall was determined by applying small drops of either bromothymol blue or chorophenol red, in a CO_2-free atmosphere saturated with water vapour, to unwashed material freshly dissected from the upper part of the oviduct.

3. RESULTS

(*a*) *Architecture of the nidamental gland*

Figure 1 illustrates the anatomy of the nidamental gland. The functional unit of the D-zone (figure 2) consists of a secretory tubule; a secretory duct; a

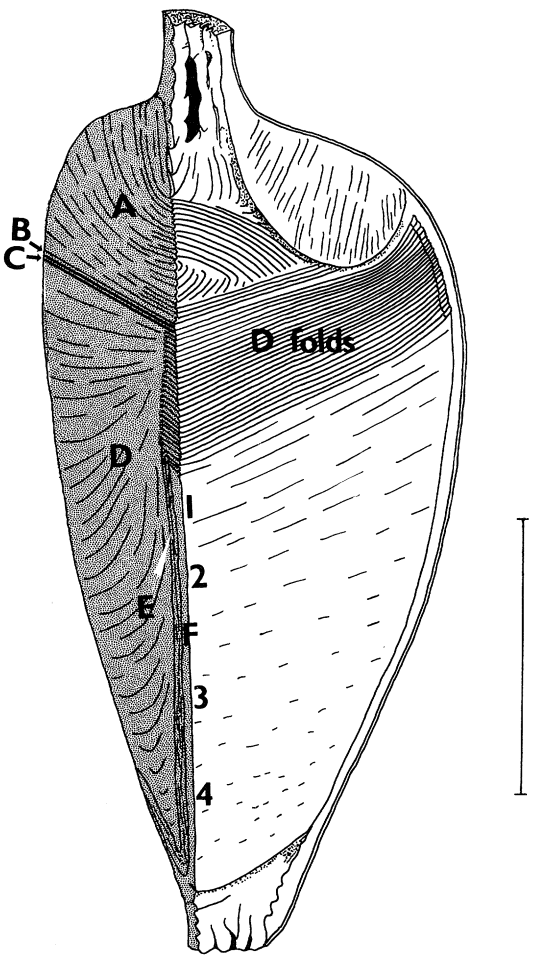

Figure 1. Semidiagrammatic view of approximately one quarter of the oviducal gland with vertical longitudinal cut surface shaded showing the distribution of glands A–E. The lumen of the gland is shown to the right with the more superficial zones of glands F_1–F_4. The anterior oviduct is uppermost. The D-zone grooves lie between the D folds which encircle the whole gland. The outline of the drawing after Metten (1939) with detail added from SEM observations. Reproduced from Knight & Feng (1992) with permission from Plenum Press Journals. Scale bar 20 mm.

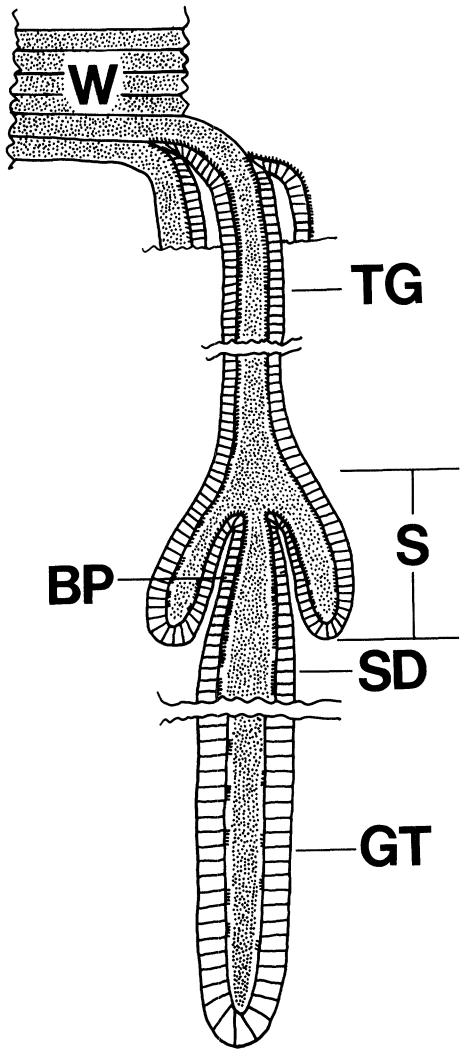

Figure 2. Diagram illustrating the functional unit of the D-zone gland. A long and non-coiled glandular tubule (GT) passes its secretion to a secretory duct (SD). From this the secretion passes between two baffle plates (BP) which lie at an angle to form the spinneret (S). From here the secretion passes apically through the transverse groove (TG) to give rise to a single lamella of the white egg case (W). The glandular tubule is approximately 60 μm in diameter.

spinneret containing the baffle plates (Knight & Feng 1992); and the transverse groove. Individual D-zone secretory tubules are 6–12 mm long and approximately 60 μm wide. A single row of approximately 150 tubules is connected to each transverse groove in each half of the gland. About 30 rows of tubules occupy approximately 75% of the volume of the gland and secrete approximately 90% of the thickness of the egg capsule wall. Each has a simple columnar epithelium containing glandular cells interspersed with non-glandular ciliated cells (Rusaouën 1978). The secretory cells of the D-zone have the characteristic appearance of cells specialized for protein secretion: their nucleus contains a large nucleolus and little heterochromatin; there is an extensive rough endoplasmic reticulum; a large Golgi stack and apical microvilli; and the cytoplasm is packed with numerous approximately spherical secretory granules about 2 μm in diameter. The marked junctional complex and extensive interdigitations of the lateral membranes indicate that this epithelium is probably also actively secreting ions (see Berridge & Oschman 1972).

(*b*) *Secretion of the egg capsule wall*

When first formed from material emerging from the transverse grooves (Knight & Feng 1992), the egg capsule wall has a white opalescence and is still plastic. In the oviduct, it quickly develops into what is usually described as the final egg capsule, becoming much more transparent and slowly darkening to a pale horn colour. After it is shed, the capsule continues to darken over a period of days.

Electron micrographs of sections of this gland show that collagen secretion in this system can be divided into a number of distinct stages: (i) collagen assembly within the *trans* cisternae of the Golgi apparatus; (ii) formation of storage granules at the *trans* face of the Golgi; (iii) maturation of the storage granules; (iv) merocrine secretion of the mature granules and their coalescence to produce a strand of secreted material within the lumen of the gland; (v) transport of the strand to the transverse grooves and initiation of fibrillogenesis; and (vi) formation of the white capsule and its transformation into the final clear capsule.

We have studied in detail the macromolecular arrangement of the collagen at each of these stages and can recognize six different liquid crystalline phases which we tentatively characterize in table 1. We now describe in detail the appearance and transformation of these phases during the different stages of secretion.

(i) *Collagen assembly within the trans cisternae of the Golgi apparatus*

The cisternae of the extensive endoplasmic reticulum of the D-zone secretory cells contain a loose and irregularly orientated meshwork of fine filamentous material. This is thought to represent the anisotropic phase (Collings 1990) of the lyotropic liquid crystalline system described below.

Table 1. *Different liquid crystalline phases of collagen in the nidamental gland and egg capsule*

Phase I:	a poorly ordered micellar phase (figures 5, 6 and 20)
Phase II:	transversely banded, smectic A or lamellar phase (figures 4–6, 8, 9 and 15–17)
Phase III:	cholesteric mesophase without transverse banding (figures 10 and 14)
Phase IV:	hexagonal columnar phase (figures 11–13, 19 and 23)
Phase V:	a second poorly ordered micellar phase (figure 21)
Phase VI:	the highly ordered fibrils of the egg capsule (figures 21, 22, 24 and 25)

Parts of the flattened *trans* cisternae of the Golgi apparatus appear to contain material with a distinct transverse centrosymmetric banding pattern (D period = 34 ± 3 nm) revealed by a negative staining effect in material stained with the Barka & Anderson (1962) method for acid phosphatase (figure 3). The positive stained equivalent was seen in material stained with uranyl acetate and lead citrate after routine fixation in glutaraldehyde and formaldehyde buffered with phosphate or cacodylate (figure 4). The appearance of this material was very similar to that of the transversely banded material (phase II) seen in developing granules (table 1). The latter material had the appearance of a liquid crystalline phase and it is likely that the banded material in the Golgi cisternae is also liquid crystalline. The mobility of the liquid crystalline phase would permit its movement through the Golgi cisternae while retaining the longitudinal registration of molecules. The cisternae of the Golgi apparatus did not appear to contain any phase II material (table 1) but the narrowness of these structures made it difficult to be certain about this.

(ii) *Formation of storage granules*

Granules with a range of diameters up to 2 μm are seen close to the *trans* cisternae in the region of the cell enclosed by the Golgi apparatus. These probably represent developing storage granules. They give a reaction for acid phosphatase and remain connected to the *trans* face of the Golgi apparatus by means of narrow, somewhat convoluted tubules while they increase in size, probably receiving contents of the Golgi cisternae via the tubules (Feng & Knight 1992). Coated pits were found in the limiting membrane of developing granules and may coat as much as half of the developing granule membrane. The material within the developing granules appeared to exist in two phases: a transversely banded phase (phase II; figures 5, 6 and 8) and a poorly ordered phase (phase I; figures 5 and 6). The transversely banded phase (D period = 33 ± 3 nm in positively material; 32 ± 3 nm in material stained with the acid phosphatase method) was indistinguishable from that seen within the Golgi cisternae. This phase was most clearly seen at the very edge of developing granules (figures 5 and 6) and may represent a tangential orientation of molecules at a hydrophilic–hydrophobic interface. A similar suggestion would account for the orientation of this material in the Golgi cisternae. The banding pattern was centrosymmetric with the D period consisting of a light band approximately 20 nm wide and a dense band 15 nm wide in positively stained material. Irregularly spaced fine filaments appear to run through the light bands with orientations roughly perpendicular to the banding pattern and may represent triple helical segments of individual collagen molecules. In grazing sections of developing granules, the dense transverse bands appeared to run continuously for up to 450 nm and frequently ended in disclinations. As disclinations are typical of liquid crystals (Collings 1990) their presence suggests that this phase is liquid crystalline. The transverse banding together with the irregularly spaced longitudinal filaments suggest that the collagen molecules were in longitudinal register but without apparent transverse order. The latter configuration is thought to occur in the gap zone in type I collagen fibrils (Parry 1988) and in both gap and overlap zones in the $3\alpha_1$ collagen, elastoidin (Woodhead-Galloway & Knight 1976; Woodhead-Galloway *et al.* 1978). The banding pattern (phase II) did not appear as sharp as that of the phase VI fibrils of the egg capsule described below and did not show the alternation of broad and narrow light bands. The detailed molecular arrangement of this phase is unknown but a smectic A or lyotropic lamellar phase (Collings 1990) or the finger print texture of a large pitch cholesteric would account for the transverse banding and the irregularly orientated fine filaments in the light bands.

Phase I material made up the bulk of the developing granules. This appeared to consist of dense granules with a diameter of approximately 15 nm in positively stained material packed irregularly but with a fairly constant separation (approximately 35 nm). These dimensions are closely similar to those of the dark bands of phase II material suggesting that both phase I and II contain the same units but without lateral registration in phase I material. This appearance together with the evidence for subsequent better

Figure 3. Ultrathin section of material stained for acid phosphatase. Banded material (phase II; small arrows) with a D periodicity of approximately 34 ± 3 nm is revealed by a negative staining effect in some regions of the *trans* Golgi cisternae. Tangentially orientated material with a similar periodicity is seen in the periphery of a developing granule (broad arrow) close to the *trans* face. Scale bar 250 nm.

Figure 4. Material similar to that seen in figure 3 is demonstrated in a *trans* Golgi cisterna by a positive staining effect. Uranyl acetate (UA) and lead citrate (PbCit). Scale bar 100 nm.

Figure 5. A large number of developing granules are seen close to the *trans* face of the Golgi apparatus. Tangentially orientated banded phase II material (small arrows) is seen in the periphery of these granules. The bulk of the granule appears to contain phase I material together with some narrow, short and irregularly orientated segments of phase II material. The amorphous material at the periphery of the granule may represent transversely sectioned phase II material. A coated pit (broad arrow) is seen in the limiting membrane of the granule. UA and PbCit. Scale bar 500 nm.

Figure 6. Part of a developing storage granule. Much of the material (phase I) in the developing storage granule appears to be constructed from rather evenly spaced granules approximately 15 nm in diameter. Tangentially orientated phase II material (small arrow) is seen at the periphery of the granule. A small segment of this material (broad arrow) is seen in the centre of the granule. UA and PbCit. Scale bar 200 nm.

Figure 7. Portion of the hexagonal columnar phase (phase V) seen in a mature granule. A fine dot can be seen at the centre of the clear area in some of the hexagons (small arrows). UA and PbCit. Scale bar 100 nm.

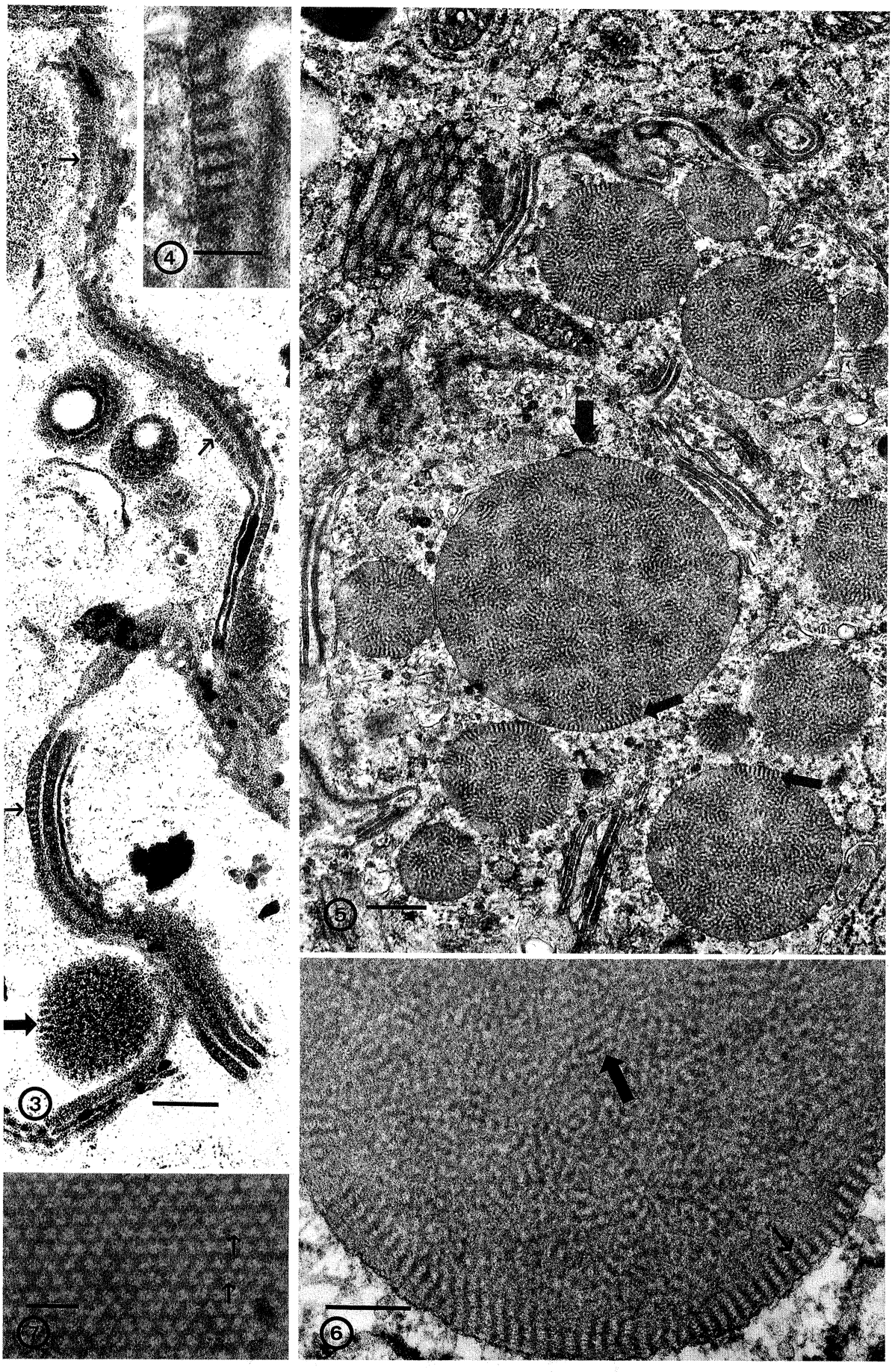

Figures 3–7. For description see opposite.

ordered lyotropic liquid crystalline phases described below, suggests that a micellar phase (Collings 1990) or two phase dispersion is likely for this material. Short, narrow irregularly orientated segments of phase II material were seen in some regions containing phase I material. These may represent a transition from phase I to phase II or vice versa. The two phases are apparently capable of existing in equilibrium with one another.

(iii) *Maturation of storage granules*

A graded series of appearances (e.g. figures 5, 8 and 12) suggest that granules undergo maturational changes while they are stored in the cytoplasm.

The earliest stage in the transformation of developing into mature storage granules was apparently represented by occasional granules which appeared to be largely filled with transversely banded phase II material similar to that seen in the Golgi cisternae and developing granules. These granules were usually found within a short distance of the Golgi zone. These observations suggest that phase I in the developing granules progressively organizes into the transversely banded phase II as the granules mature. Granules apparently filled with phase II material often exhibited a spiral or concentric pattern built up from a fairly regularly spaced alternation of light and dark laminae. The dark laminae contained longitudinally sectioned transversely banded material whereas the pale laminae appeared to contain transversely sectioned filaments which were considerably finer than those seen in the light laminae of phase III material (table 1). The spiral pattern of alternating light and dark laminae of phase II material was closely similar to that of the mature spiral granules (phase III). The mature spiral granules, however, did not show transverse banding and had coarser transversely sectioned filaments in the light laminae. These observations are compatible with the suggestion that phase I material transforms into phase II which then becomes organized into a spiral pattern before undergoing an alteration of molecular packing to give rise to phase III material arranged in the same spiral pattern.

Most granules seen in the apex of the D-zone secretory cells were of the type described as 'grains spiralés' by Rusaouën (1978; 'spiralled grains', Rusaouën-Innocent 1990*a*,*b*). Most of the material in these granules appeared to be arranged to give rise to a concentric or spiral pattern of alternating light and dark bands described above. The light bands contained rather evenly spaced, transversely sectioned fine filaments approximately 40 nm in diameter while the centre of the dark bands contained longitudinally sectioned filaments of the same diameter. The size of these filaments suggested that they represent parallel aggregates of a small number of collagen molecules. Obliquely orientated filaments were seen between the transversely and longitudinally sectioned ones. This appearance was similar to that of a cholesteric mesophase liquid crystal and has been described in a variety of biological materials including DNA, chitin-protein and cellulose as reviewed by Bouligand (1972, 1978) and is also thought to be present in a variety of collagenous systems (Giraud-Guille 1989). The spiral pattern probably represents the double twist cylinder first observed in cholesteryl benzoate liquid crystals (Collings 1990), but modified by being constrained within a spherical granule. These observations suggest that phase III is a cholesteric mesophase. The loss of transverse banding as phase II transformed into phase III suggested that this transformation resulted from a loss of longitudinal molecular register. The observation that phase III appears to be constructed from 40 nm filaments or protofibrils suggests that this loss of longitudinal register may be accompanied by a lateral aggregation of molecules into small protofibrils.

The hexagonal columnar crystalline phase (IV) was seen in mature storage granules in the apex and elsewhere in the cell. Some storage granules appeared to be almost entirely packed with crystallites of this

Figure 8. A granule which appears to be almost entirely packed with phase II material. This is thought to represent a transitional stage between the developing granule (figures 5 and 6) and the mature granule with the double twisted cholesteric mesophase arrangement (figure 10; phase III). UA and PbCit. Scale bar 0.5 μm.

Figure 9. A granule similar to that seen in figure 8 which appears to be largely filled with phase II material. A concentric pattern of rather evenly spaced light and dark bands is seen similar to that in figure 10 but with the banding seen in phase II material. The pale bands appear to be practically amorphous at this magnification and are thought to represent transversely and obliquely sectioned ribbons of phase II material. The granule is thought to represent a transitional stage between the developing and the mature granule. UA and PbCit. Scale bar 0.5 μm.

Figure 10. A mature granule largely filled with phase III material but with small quantities of what appears to be phase IV material. The pattern of alternate light and dark bands is similar to that seen in figure 9 but the constituent material is not D periodic and is seen to be composed of fine protofibrils. UA, phosphotungstic acid (PTA) and PbCit. Scale bar 250 μm.

Figure 11. A mature granule containing both phase III (broad arrow) and columnar hexagonal phase IV material (narrow arrow). The hexagonal columnar material is found within a lattice defect in the phase III material. UA, PTA and PbCit. Scale bar 250 nm.

Figure 12. A mature granule which appears to be largely filled with phase IV material but with a small quantity of phase III material visible in the periphery of the granule on the right hand side. The bulk of the contents appear as two hexagonal crystallites with a lattice dislocation between them. UA, PTA and PbCit. Scale bar 0.5 μm.

Figure 13. When PTA is omitted the phase IV pseudocell has the same spacing as in material stained with PTA but appears as a dark hexagon with a light centre. What appears to be a view down the 001 plane (arrow) and several lattice defects can be seen. UA and PbCit. Scale bar 0.5 μm.

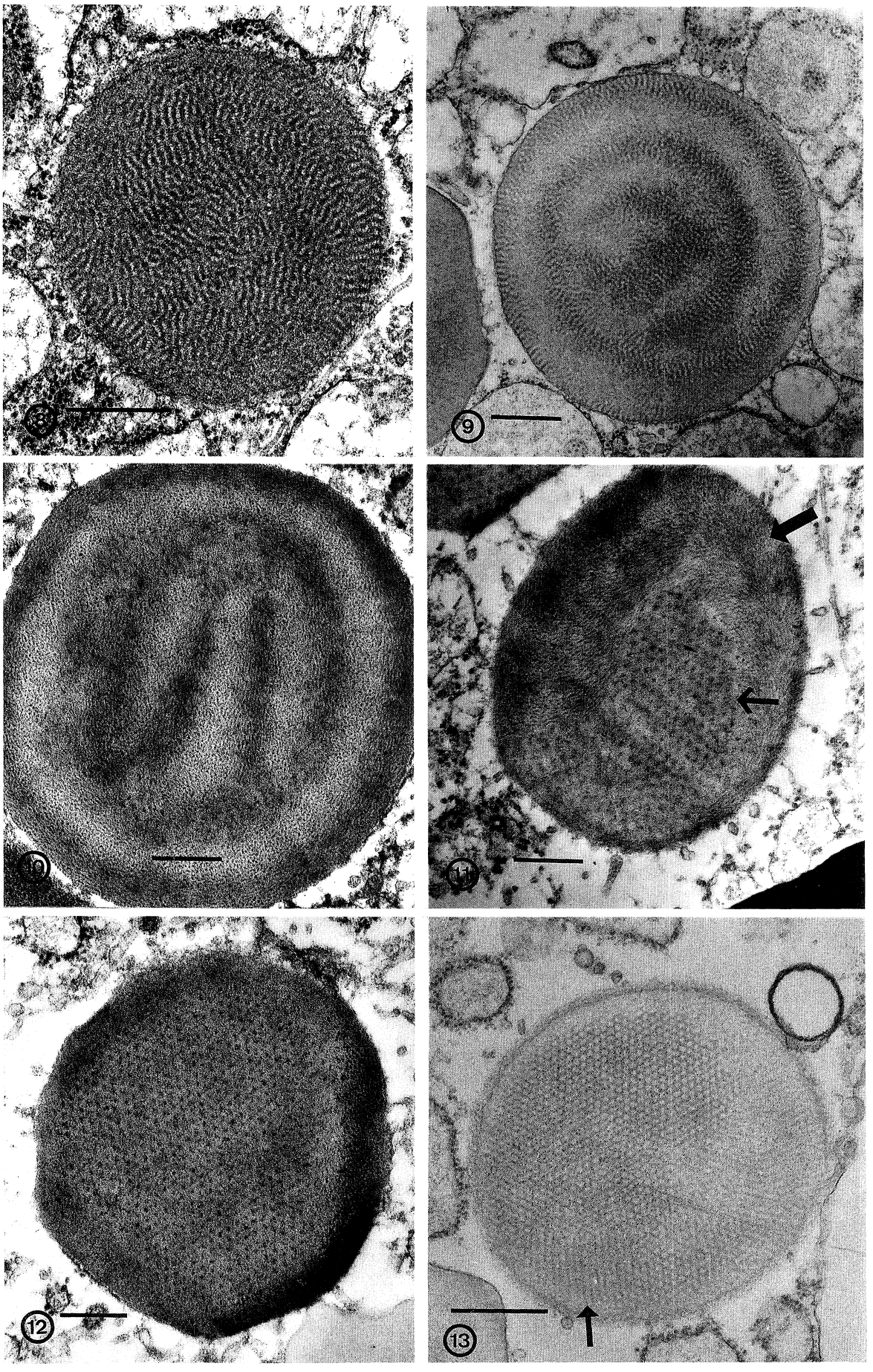

Figures 8–13. For description see opposite.

material (figures 12 and 13). The appearance of this phase depended on the method of staining (figures 12 and 13). In ultrathin sections stained in uranyl acetate and lead citrate without phosphotungstic acid, the unit cell of the transversely sectioned crystallites was composed of a dense hexagonal ring with a light centre (figures 7 and 13). Filtered images of these showed that each central lightly staining zone was surrounded by six regions of high density (figure 23) located at the mid-points of the triangles formed by the centres of adjacent light zones. These subunits were also seen in some regions in the original electron micrographs (figure 19). The hexagonally arranged light zones were spaced 42 ± 3 nm apart, which was somewhat larger than that of D period of phase II but close to that of phase VI (35 ± 1 nm). A small central dense dot was sometimes seen in the light centres of the hexagons (figure 7) after uranyl acetate and lead citrate staining. This appeared to represent the cross section of a fine filament seen as a fine interperiod line in crystallites apparently sectioned parallel to the 101 plane. Coherent crystallites varied in size from quite small to about 1 μm in diameter, and appeared to be packed together rather irregularly. Lattice dislocations were frequent. Images of what appeared to be views of the 100 and 101 projections were seen in longitudinally sectioned crystallites. The columnar nature of the crystallite was confirmed by observing serial ultrathin sections with a thickness of approximately 60 nm judged by interference colour. In these series, the hexagonal pattern in transversely sectioned crystallites could be followed from section to section for up to 540 nm. The series also demonstrated that crystallites sometimes abut one another at an angle of 90°.

A progressive bending of the Z axis of the crystal was often seen in crystals sectioned perpendicular to the 0 plane. This and the numerous disclinations noted in these crystals suggest that this phase is liquid crystalline. This phase closely resembles the numerous irregularly orientated hexagonal columnar crystallites observed by Livolant (1991) in freeze fractured concentrated solutions of DNA.

A different though related staining pattern was seen in hexagonal columnar crystals in ultrathin sections additionally stained in phosphotungstic acid (figures 11 and 12). Here the pattern of dense hexagons appeared to be replaced by a hexagonal pattern of dense granules (diameter approximately 15 nm) with the same spacings as in material stained only in uranyl acetate and lead citrate. Views perpendicular to the 0 plane suggested that the dense granules seen in cross section in the hexagonal array in phosphotungstic acid stained material represented continuous filaments. They may represent an intensified staining of the faint dot seen after uranyl acetate and lead citrate staining. It is not known whether the two different staining patterns represent a negative and positive staining of the same component or a differential staining of two components such as the globular and triple helical, or hydrophobic and hydrophilic regions of the molecule.

Phase IV granules were smaller (mean diameter 1.1 ± 0.4 μm) than those of spiral phase III. The outline of the granule was sometimes somewhat polygonal, the sides following the lattice boundaries of the enclosed crystallites. A graded series of appearances suggested that phase III material transforms into phase IV or vice versa. Most spiral granules contained at least a small quantity of phase IV material whereas most granules containing large quantities of phase IV material still contained a little phase III material in their periphery. The hexagonal columnar phase was sometimes seen in a lattice dislocation of the phase III material as reported in DNA (Livolant & Leforestier 1992). The apical cytoplasm of the cell contained granules with a range of compositions from practically all phase IV material to practically all phase III material, suggesting that granules containing both phases are secreted from the cell.

(iv) *Merocrine secretion of the mature granules*

Ultrastructural appearances of D-zone cells in nidamental glands actively engaged in the secretion of the egg capsule suggested that the storage granules were shed by classical merocrine secretion. The vast majority of the storage granules in the apical cytoplasm contained a variable proportion of phase III and IV material. These granules appeared to come to lie under the apical plasma membrane. The cytoplasm between the limiting membrane of the granule and the cell membrane appeared to thin and then rupture. As soon as the limiting membrane surrounding the granule ruptured, the contents of the granule appeared to transform rapidly from phase III and IV back to a mixture of phase II and phase I; all granules which had lost all or part of their limiting membrane contained only phase I and II material (figures 15 and

Figure 14. Part of a mature granule showing phase III material which has the appearance of a cholesteric mesophase. UA, PTA and PbCit. Scale bar 100 nm.

Figure 15. Two granules (arrowed) at the apical surface of the cell which appear to have been fixed in the act of merocrine secretion apparently contain only phase II material. The vast majority of the granules found in the apex of the cell are mature granules containing a mixture of phase III and IV material. The simplest hypothesis to account for this is that the contents of mature granules show a rapid transition to phase II as soon as the limiting membrane is breached. UA and PbCit. Scale bar 500 nm.

Figure 16. A section through the lumen of the lower (proximal) part of a tubule shows the coalesced strand of material (B) and the contents of a secreted granule (A) which has not yet coalesced with B. The granule appears to be largely filled with phase II material closely resembling that seen in the grazing section of the coalesced secretion. The transverse order in this material does not appear to be as good as in phase VI. The lumen contains numerous myelin figures. In two instances these appear to adhere to the membrane of a cilium (arrowed). UA and PbCit. Scale bar 100 nm.

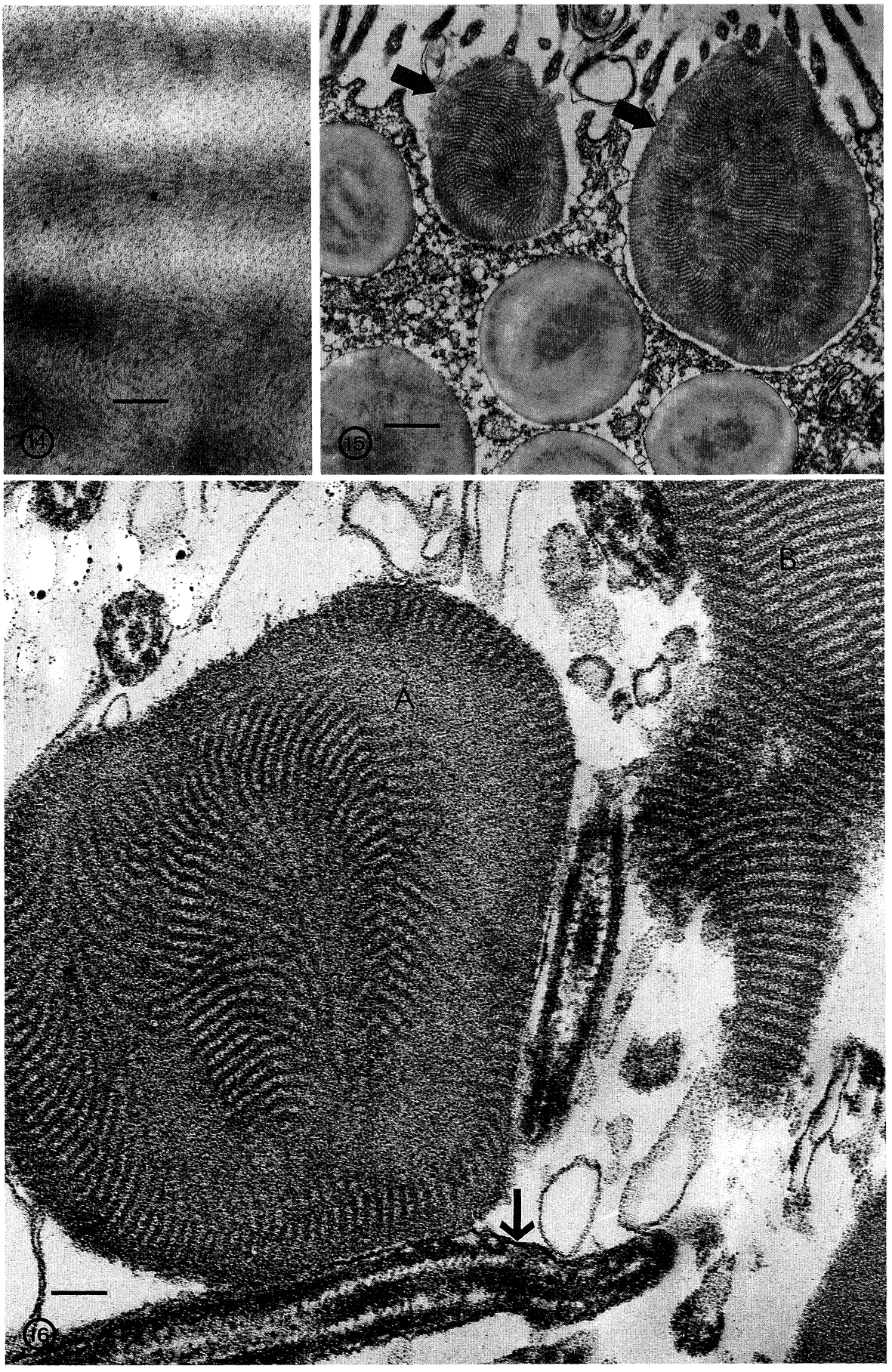

Figures 14–16. For description see opposite.

20). There was some suggestion that phase II material formed first and subsequently transformed into a mixture of phase II and phase I; generally, the further secreted granules were away from the cell surface the more phase I and the less phase II material they contained. Loss of the limiting membrane of the granule and part of the plasma membrane during secretion may result in the numerous myelin figures seen in the lumen of the actively secreting gland (figures 16 and 20). Appearances suggest that these may be recycled by adhering to microvilli and flagella. TEM and SEM suggest that the secreted granules coalesce with the strand of secreted material as it passes along the lumen of the tubule towards the spinneret. The secreted material does not appear to fill the lumen completely and is probably moved towards the spinneret partly by ciliary action, there being no smooth muscle or myoepithelial cells in the wall of the tubule (see Knight & Feng 1992). The material in the lumen of the lower (proximal) part of the glandular tubule was indistinguishable from that in the secreted granules which coalesced to give rise to it (figures 16 and 20). Both contained phase I material with some of the phase II material tangentially orientated at the surface of the material. The phase II material on the surface of the coalesced strand is seen to be orientated tangentially in transverse sections and predominantly parallel to the long axis of the secreted strand in grazing sections. The latter probably correlated with the weak birefringence of the secreted material in this region. This may arise as flow birefringence which then defines the orientation for liquid crystallization. A similar suggestion has been made for the orientation of material flowing through the spinneret in this system (Knight & Feng 1992). In grazing sections of the secreted material within the lumen of the tubule, the transverse bands of the phase II material ran for considerable distances often ending in disclinations (figure 17). Fine irregularly spaced filaments similar to those in developing granules were seen running perpendicular to the transverse bands in this situation.

(v) *Formation of phase VI fibrils*

Secreted material flows on from the tubules through the secretory ducts to the spinnerets in the base of the transverse grooves where orientation of the orthogonal laminae is thought to be defined (Knight & Feng 1992). The secreted material in the lumen of the proximal part of the tubule appeared to be composed of phase I and II material. As the material flowed towards the spinneret there appeared to be a progressive decline in the amount of phase I and phase II material coupled with the appearance of a second poorly ordered phase (phase V). The latter appeared to consist of dense rings, polygons or hexagons with light centres sometimes with a dense central dot as in the hexagonal columnar phase. These rings appeared tightly but irregularly packed together with a fairly constant centre to centre separation of about 40 nm. This spacing and appearance was remarkably similar to that of the hexagonal columnar phase suggesting that the molecular arrangement was similar but that phase V did not show the regular uniaxial packing into columns. Virtually all the material within the spinneret had this appearance. Here the transmission electron microscope gave little indication of the preferred orientation revealed by the polarizing microscope (Knight & Feng 1992). The ultrastructure of phase V material and the existence of other liquid crystalline phases in this system suggested that this represents a micellar phase. The observation that phase V was similar to a negative image of phase I was compatible with the suggestion that phase V represents a micellar arrangement with reversed hydrophilic polarity to phase I. If phosphotungstic acid stains the hydrophilic regions and osmium/uranyl acetate/lead citrate the hydrophobic regions, phase I may represent micelles with hydrophobic centres

Figure 17. Grazing section of coalesced material in the lumen as in figure 16 showing two different types of disclination (arrowed). UA and PbCit. Scale bar 200 nm.

Figure 18. Tangentially orientated material (broad arrow) lies at the surface of the coalesced material in the proximal part of the tubular gland while the deeper material shows some phase I material and small irregularly orientated segments of phase II material (narrow arrow). UA and PbCit. Scale bar 200 nm.

Figure 19. High magnification micrograph of an ultrathin section of columnar phase material stained with UA and PbCit. The dense hexagonal ring appears to be constructed from six subunits (arrows) best seen in the reconstructed image (figure 23). Scale bar 50 nm.

Figure 20. Proximal part of the tubule. Secreted material (M) which forms the coalesced strand appears to be constructed largely from phase I material and is closely similar to the contents of the granule (G) whose limiting membrane (arrowed) is thought to have recently ruptured. Microvilli, cilia and numerous myelin figures are seen in the lumen. UA and PbCit. Scale bar 1 μm.

Figure 21. TS. white egg capsule. The material appears to consist of two phases: Fibrils similar to those seen in the final egg case (phase VI; broad black arrow) and micelles (phase V) in between them which appear to consist of a dense ring with a light centre in which a dense central dot (tip of white arrows) is sometimes seen. The high degree of transverse order in the fibril can be seen to the right of the black arrow. The dense transverse bands of the fibrils appear to run continuously from fibril to fibril (see text). UA, PTA and PbCit. Scale bar 100 nm.

Figure 22. Final egg case. This appears to constructed almost entirely from phase VI fibrils. These appear longitudinally sectioned in most of the micrograph but are obliquely sectioned in a narrow strip at the bottom. Material fixed in a solution containing 1% glutaraldehyde and 3% paraformaldehyde and 1% tannic acid. UA, PTA and PbCit. Scale bar 100 nm.

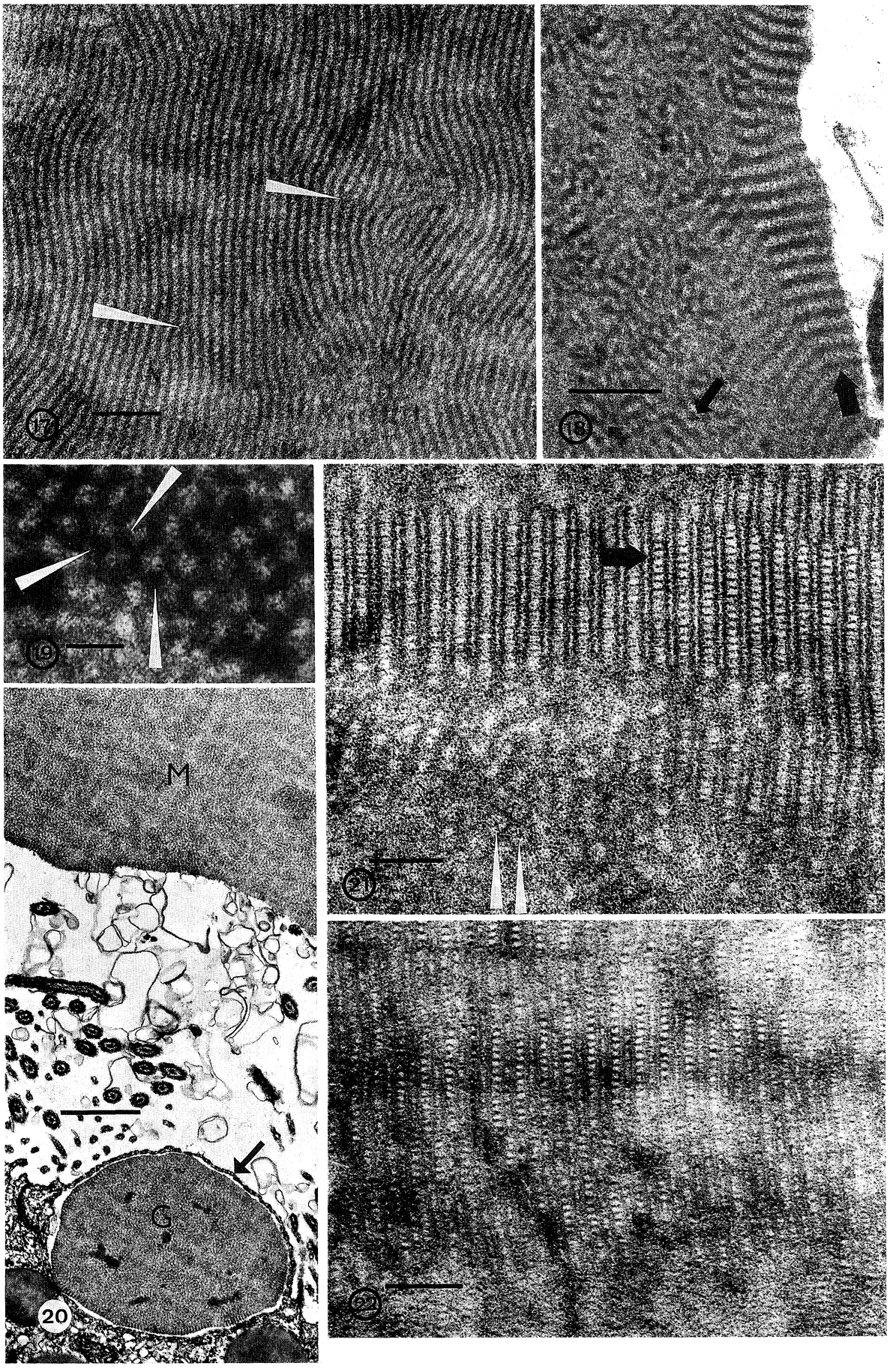

Figures 17–22. For description see opposite.

while phase V micelles may have hydrophilic centres.

The phase VI fibrils described below are first found within the transverse grooves distal to the spinneret (Rusaouën-Innocent 1990) but were present only in small numbers in this region. Much of the formation of the phase VI fibrils appeared to take place after the material had left the transverse folds and moved in a posterior direction for approximately 150 μm down the lumen of the nidamental gland. The laminae of the newly formed white egg case in this region contained large numbers of type VI fibrils with a small diameter. The fibrils appeared to grow in diameter as the laminae moved further down the lumen of the gland. There appeared to be a progressive increase in the number of phase VI fibrils accompanied by a decrease in the amount of phase V material as the material moved distally through the transverse grooves to become the laminae of the white and then the clear egg capsule. This suggests the progressive conversion of the micellar phase V into phase VI fibrils.

(vi) *Transformation of the capsule from white to clear*

Each lamella of the thickest layer (L_2) of the egg capsule is secreted from a single transverse groove and consists of five laminae (Knight & Feng 1992). Each lamina appears to be built from fibrils with a uniaxial orientation parallel to the lamina. The orientation of fibrils in the successive laminae of a single lamella increases by 45° to give an orthogonal arrangement similar to that of plywood (Knight & Feng 1992). The laminae of the white egg capsule appeared to be constructed from parallel orientated highly ordered fibrils (phase VI) separated by small quantities of phase V material (figure 21). In some cases the hexagons of the phase V material appeared to lie in register with the transverse banding of adjacent phase VI fibrils.

The existence of two phases with different refractive indices probably accounts for the opalescence of the white capsule. The ultrastructure of the highly ordered phase VI fibrils has been described (Knight & Hunt 1974, 1976, 1986). The fibrils show a transverse centrosymmetric banding pattern (D period 37 nm) which, in positively stained material, appears to consist of an alternation of narrow (7 nm) and broad (12 nm) light bands separated by dense bands (9 nm wide). Negative stain penetrates equally into the broad and narrow bands and is strongly excluded from the dense bands (Hunt & Knight 1974). The dense bands appeared to run continuously from fibril to fibril with exact registration between adjacent fibrils or with what appeared as disclinations or lattice dislocations (figure 21) at the interface between fibrils. The structure of the broad light bands is crystalline showing a body centred tetragonal arrangement with a 11 nm pseudocell (Knight & Hunt 1976). Kinked molecular segments arranged at an angle of approximately 25° to the long axis run through the narrow light bands to connect the two body centred faces of the tetragonal pseudocell in adjacent broad light bands (Knight & Hunt 1986). Filtered images prepared from longitudinally sectioned fibrils in the white egg case gave good views of this structure projected onto the 100 and 101 planes (figures 24 and 25). Although the size of the D period was similar in phase VI, the latter showed an alternation of light and narrow dark bands together with a very high degree of transverse order not seen in phase II. The existence of a sharp centrosymmetric transverse banding pattern, the alternation of transverse bands of high density which exclude negative stain with bands of considerably lower density and the possibility that the structure contains highly ordered bands separated by less ordered bands (Knight & Hunt 1974, 1976, 1985) all suggest a lamellar liquid crystalline phase (Collings 1990) for these fibrils.

The L_2 laminae of the clear egg case appeared to be composed almost entirely of parallel orientated phase VI fibrils closely packed together with almost no additional material between them (figure 22). The existence of a single phase and therefore a uniform refractive index probably accounts for the high degree of transparency of the clear capsule as it may do in the mammalian cornea (Quantock *et al.* 1991; Benedek 1970). The continuity of the dense transverse bands from fibril to fibril suggests that each lamina of L_2 can be regarded as a single liquid crystal. The progressive decline in the thickness of the L_2 lamellae from formation in the transverse folds through the white capsule to the final clear capsule may result from a loss of water as the irregularly packed micelles (phase V) transform into the highly ordered fibrils (phase VI). There would appear to be a considerable increase in both lateral and transverse order as this occurs and this is commonly seen as lyotropic systems loose water (Collings 1990). The transition may involve the conversion of a hexagonal micelle (phase V) to a non-planar hexagonal unit (Galloway 1986) with closely similar dimensions.

The arrangement of the phase VI fibrils in the laminae of the orthogonal system with an angle of 45° between the fibril axis in successive laminae may represent cholesteric liquid crystallization at a higher level of organization (Knight & Feng 1992). The extreme insolubility of the collagen of the final capsule, its resistance to swelling in lyotropic agents, and a progressive increase in the half shrinkage temperature from white to final egg capsule (Knight & Feng unpublished) suggests that the phase VI fibrils undergo a progressive intermolecular covalent cross-linking.

(*c*) *Solubility of the collagen in D-zone storage granules*

Brief extraction of unfixed cryostat sections with 0.1 M acetic acid removed all the material staining with Mallory's aniline blue from the storage granules, but produced no apparent decline in the intensity of staining of either the small quantities of collagen seen between the gland tubules or of the tubule basement membrane. This suggests that there is an absence of intermolecular covalent cross-links in the stored collagen. The solubility of the collagen was confirmed by testing 0.1 M acetic acid extracts of the D region of

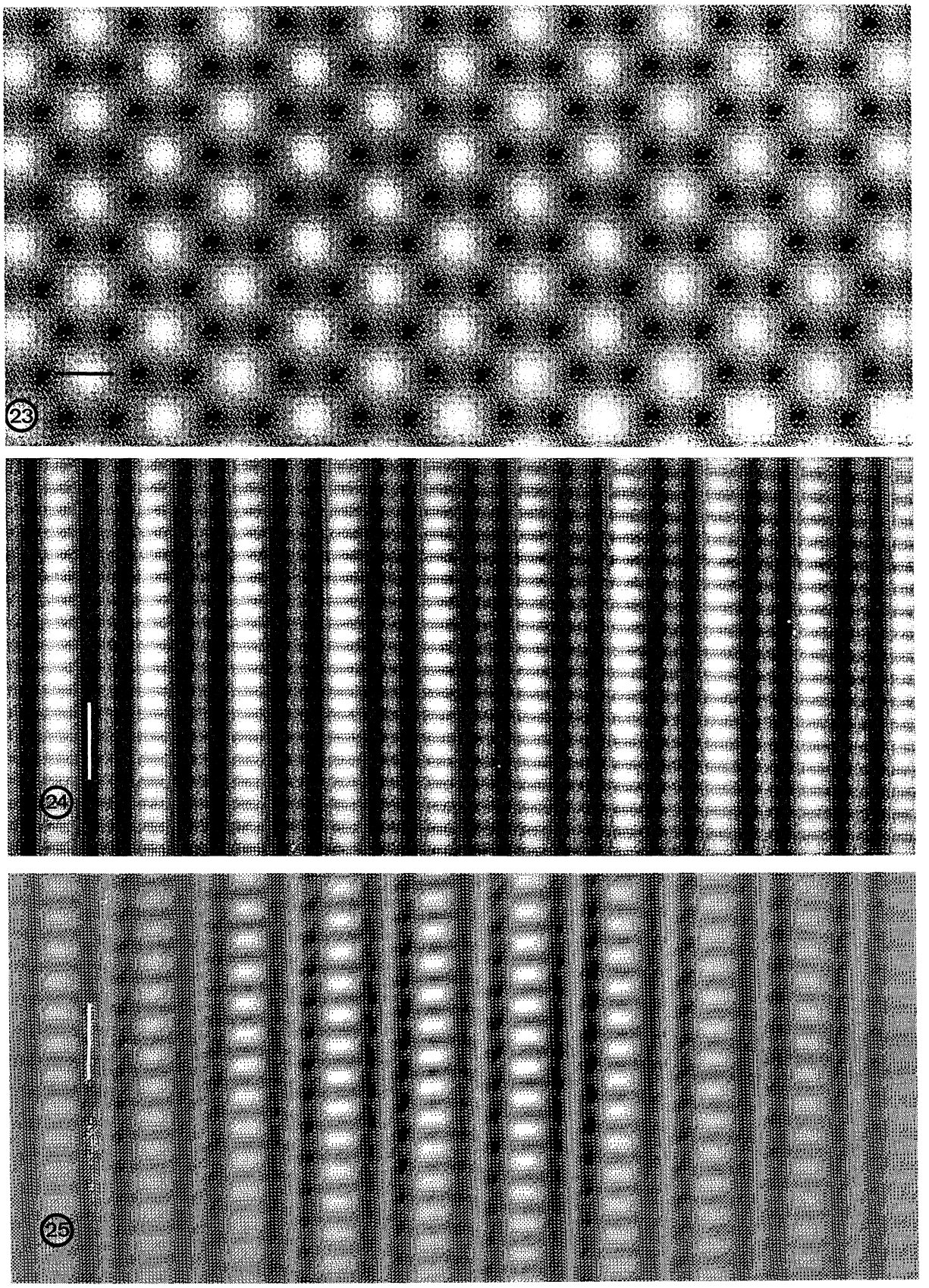

Figure 23. Reconstructed image of the hexagonal columnar phase (IV) prepared from a micrograph stained with UA and PbCit. Each hexagon contains six dense subunits. Scale bar 30 nm.

Figure 24. Reconstructed image of a longitudinally sectioned fibril (phase VI) from the white egg capsule stained with UA, PTA and PbCit. Projection 2 (Knight & Hunt 1976). Scale bar 30 nm.

Figure 25. As figure 24 but showing project 1 (Knight & Hunt 1976). Scale bar 30 nm.

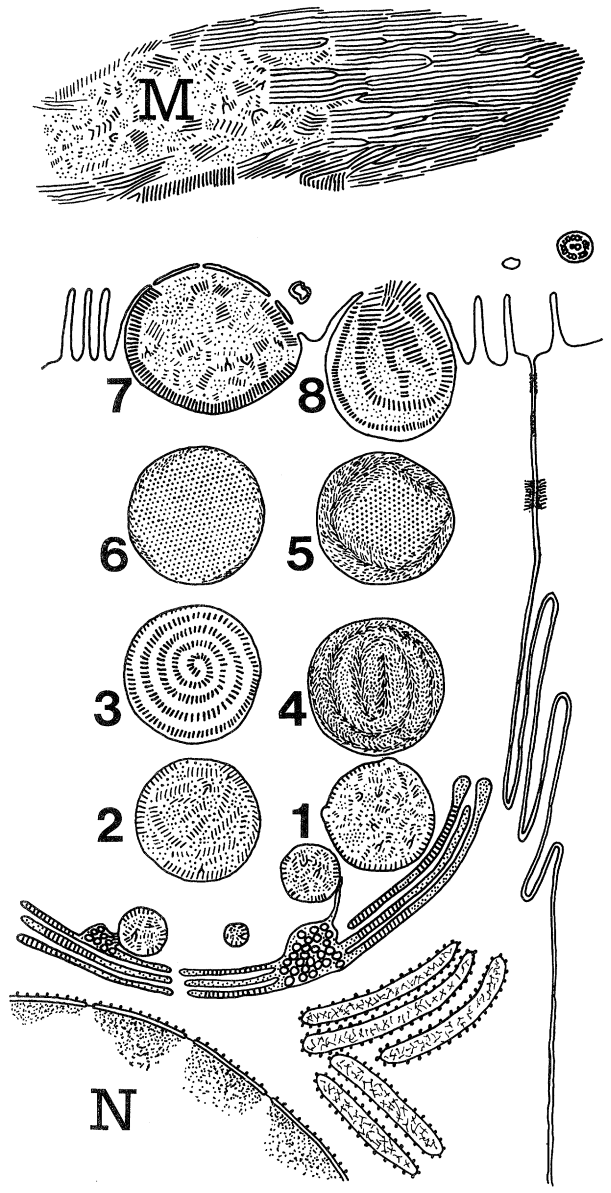

Figure 26. Diagramatic drawing of a part of a secretory cell in the proximal part of a D-zone secretory tubule to illustrate the tentative scheme for the sequence of changes thought to occur during storage and secretion of the (pro)collagen. Nucleus (N). The ER contains the anisotropic phase. The Golgi cisternae contain some phase II material. 1, Developing granules containing phases I and II. 2, Developing granule containing a higher proportion of phase II. 3, Granule containing spirally orientated phase II material. 4, Double twisted cholesteric hexagonal columnar phase (IV) and some phase II material. 5, Granule containing both cholesteric (phase III) and phase IV material. 6, Granule containing mainly phase IV material. 7 and 8, Granules undergoing merocrine secretion with consequent reversion to phases I and II.

the nidamental gland with Sircol/picric acid. The extracted collagen could be partly purified by precipitation with 20% saturated ammonium chloride and further purified by DEAE Sephadex chromatography. The second UV absorbing peak (elution volume 150 ml) emerging from the DEAE column gave an intense reaction with the Sircol assay, demonstrating that it contained the bulk of the collagen. SDS polyacrylamide gel electrophoresis of fractions corresponding to this peak gave a single band at approximately 44 kDa thought to correspond to the α chain of the collagen. The same band and a second band at about 40 kDa were conspicuous in extracts of the white egg capsule prepared with or without mercaptoethanol reduction. The purified collagen formed a gelatinous precipitate when the pH was raised to 5.8 which, once formed, appeared completely insoluble in 0.1 M acetic acid. The purified collagen could also be precipitated by dialysis against 0.1% ATP in distilled water. Negative staining the latter precipitate with 2% phosphotungstic acid revealed short lengths of banded fibrils (D period 44 ± 3 nm) with an appearance similar to that of phase II material.

(*d*) *Stability of isolated D-zone granules*

The region containing D-zone tubules was dissected from the nidamental gland and cut into small pieces with razor blades before being dispersed in a small ground glass homogenizer. The isolated D-zone granules prepared in this way were stable in distilled water, 2% sodium chloride or 2–10% polyethylene glycol for periods of at least 12 h.

4. DISCUSSION

(*a*) *Liquid crystalline phases during the storage, secretion and fibrillogenesis of egg capsule collagen*

Our ultrastructural data suggest a series of lyotropic liquid crystalline phases as the collagen of the D-zone secretory cells is assembled in the Golgi cisternae, then stored within the cell, secreted into the lumen of the tubule and assembled into the lamina of the egg case. It is unlikely that the distinct appearance of material in different storage granules represented different biochemical constituents, because the laminae of the egg case produced from this secreted material appeared to be constructed very largely from a single type of highly ordered fibril. It seems unlikely that such highly ordered fibrils could be assembled from a mixture of constituents secreted in stoichiometric quantities from several types of granules with variable composition. It is important to bear in mind that the effect of fixative solutions on liquid crystalline phases in this system is unknown so one cannot assess the extent to which the patterns observed might be artefacts of specimen preparation. It is, however, encouraging that similar appearances are obtained in material fixed in glutaraldehyde–formaldehyde solutions in a variety of buffers including: sodium cacodylate with added sodium chloride; phosphate; and PIPES with added sucrose but no added mono- or divalent cations. In the future, further purification of the collagen may lead to the possibility of examining these liquid crystal transitions *in vitro* using polarizing microscopy and other direct physical techniques.

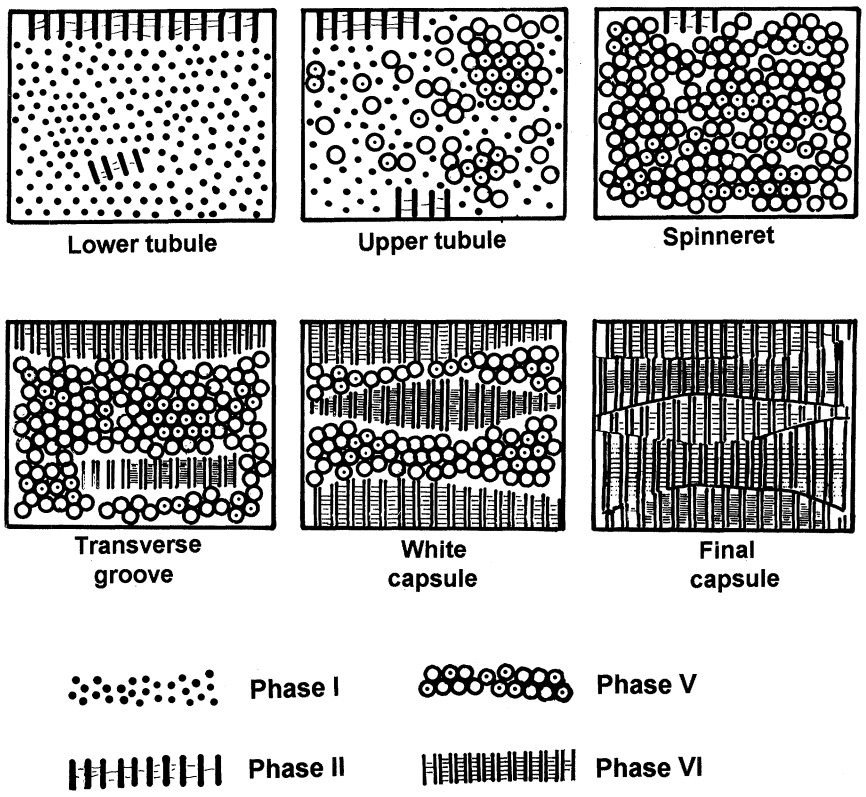

Figure 27. Tentative scheme for phase changes occurring during fibrillogenesis.

A tentative scheme for the ultrastructural changes and liquid crystal transitions in this system is summarized in figures 27 and 28 but it is possible that not all the different appearances represent thermodynamically distinct phase states. Liquid crystal transitions similar to those postulated have been produced *in vitro* in other lyotropic systems (Collings 1990) including solutions of DNA fragments (Livolant & Leforestier 1992) by changes in water content and a similar mechanism may account for the phase changes during storage and merocrine secretion in the nidamental gland. Reduction in water content during storage could be produced by a proton pump similar to those demonstrated in Golgi cisternae, lysosomes, storage granules and other vesicles (Al-Awqati 1986; Forgac 1989; Schneider 1987). The progressive difficulty in cutting ultrathin sections of the storage granules as they mature and the apparent reduction in the diameter of granules which contain predominantly hexagonal columnar (phase IV) material supports the suggestion that there is a progressive loss of water from the storage granules. The hexagonal columnar phase may represent the most compact way of storing the material within the cell.

The collagen of the storage granules was completely soluble in dilute acetic acid, demonstrating that no intermolecular covalent links had developed by this stage. Such crosslinks would certainly impede liquid crystal transitions. The acidity of the storage granule contents, produced by a proton pump, may prevent hydrogen and electrovalent bonding during storage, thus permitting subsequent phase changes and delaying fibril formation until the desired oriententation has been defined in the spinneret. In this connection it is interesting to note that the partly purified collagen from this system is precipitated when the solution is neutralized and that once formed, this precipitate is insoluble in dilute acetic acid. Hydrophobic interactions may be important in maintaining molecular associations in the liquid crystalline phases in this system (see Collings 1990).

The rapid phase changes seen when the granule membrane breaks down on secretion suggest that rehydration simply reverses the changes that have occurred during maturation of the storage granules. The fact that subsequent changes in the secreted material do not exactly parallel the changes that occur within the cell suggests that some factor additional to dehydration is responsible for fibrillogenesis in this system. Fibrillogenesis may be brought about by a change in either the ionic environment or the biochemical composition of the secreted material or both. The former possibility is indicated by the ultrastructural appearance of the epithelia of the gland tubules, spinneret and transverse grooves which suggests that they are actively involved in ion transport, possibly of sodium ions (Knight & Feng 1992). Our observations that the collagen is irreversibly precipitated when an acidic solution is neutralized and that the pH of newly secreted material is nearly neutral (pH 6.2–6.4) suggest that fibrillogenesis may be initiated by neutralization. Neutralization might permit electrovalent and hydrogen bonding which would render the material insoluble. Once the fibril was formed in this

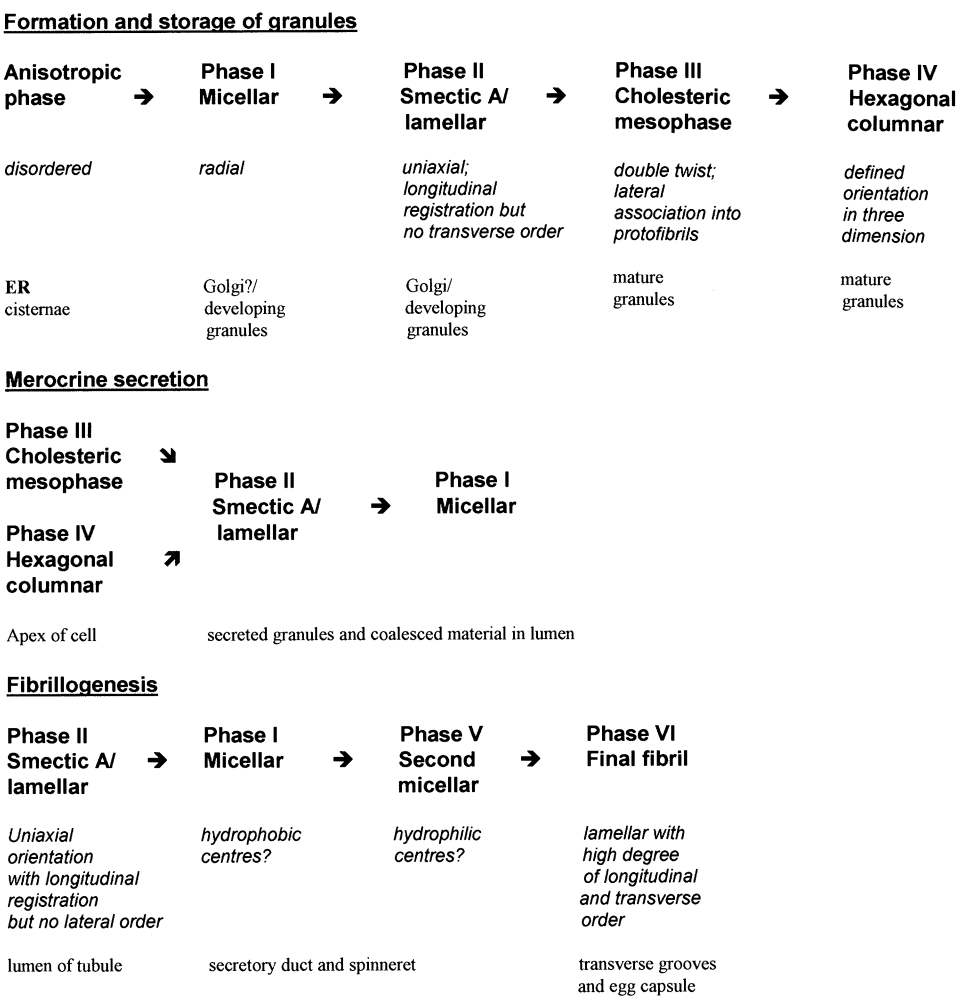

Figure 28. Tentative scheme for all phase changes in the nidamental gland/egg capsule.

way covalent stabilization by oxidative phenolic cross-linking (Knight & Feng 1992) and possibly disulphide bonds (Rusaouën-Innocent 1990*a*) would help to account for the exceptional thermal shrinkage temperature, toughness and insolubility of this material. The low density and low collagen packing fraction (Galloway 1986) of the structure we have proposed for phase VI fibrils (Knight & Hunt 1976, 1985) suggest that an extremely strong and highly permeable material (Feng & Knight 1992) is produced with the minimal use of valuable protein.

It is necessary to consider the possibility that proteolytic removal of non-helical propeptides may be involved during the secretion of this collagen as it is in other collagenous systems (Davidson & Berg 1981; Prockop *et al.* 1979). The evidence that SDS polyacrylamide electrophoresis demonstrated the same band (44 kDa) in both the purified collagen from the gland and the extract of the egg capsule suggested, however, that no detectable change in molecular mass occurs between storage and secretion. This does not rule out the possibility that post-translational proteolytic processing occurs in the endoplasmic reticulum and *cis* Golgi cisternae before storage.

Although liquid crystallization has been suggested to account for fibril orientation in a number of collagenous systems (Giraud-Guille 1989), and the assembly of type IV collagen in the lens capsule (Barnard & Gathercole (1991), liquid crystal transitions do not appear to have been described in collagens or other secreted proteins. However, Farber *et al.* (1986) concluded from a study of turbidity changes during fibrillogenesis in type I collagen *in vitro* that the pre-nucleation stage involves several steps which appear reversible while the final fibril is stable once formed. We suggest that the reversibility of the phase changes during pre-nucleation suggests that these are liquid crystal transitions. The thermal reversibility of precipitation from dilute neutral solutions of type IV collagen (Yurchenko & Furthmayr 1984) and the thermal reversibility of the lateral but not linear association of type I collagen (Gelman & Piez 1980) may be further indications of liquid crystal transitions. Another possible liquid crystal transition is seen in odontoblasts. The endoplasmic reticulum in these cells in decalcified material contains hexagonal paracrystalline arrays (Jessen 1967). We suggest that these represent a hexagonal columnar phase in the formation of the intraodontoblastic collagen fibrils reported by Ishizeki, Sakakura & Nawa (1987). The latter fibrils show a centrosymmetric pattern not unlike our phase VI fibrils. The hexagonal lattice of

type VIII collagen in Descemet's membrane in the cornea (Sawada *et al.*1990) may represent a hexagonal columnar liquid crystal. Fibrils which appear to have a similar structure to our phase II material but with a larger D period are seen in type VIII collagen in a variety situations (Edwards 1975; Henry *et al.* 1992). The arrangement of the C terminal domain in anchoring plaques in the dermal–epidermal basement membrane as described by Keene (1987) suggests a micellar liquid crystalline arrangement. The existence of a sequence of 29 hydrophobic amino acids in the carboxyterminal NC-1 domain of the α_1 chain of type X collagen (Schmid & Linsenmayer 1987) indicates that a liquid crystalline model may be appropriate for this collagen. It is also interesting to note that the model for type I collagen fibrils which Parry (1989) considers to fit X-ray diffraction data best is crimped with highly ordered straight segments of tilted collagen molecules in the overlap regions linked to one another by relatively disordered, mobile molecular segments in the gap region. The latter region has a much higher water content, lower packing fraction and lower content of imino and aromatic amino (Fraser *et al.* (1987). This model bears a close resemblance to that of the kinked phase VI fibrils and has the properties of a smectic A liquid crystal.

The use of collagens in a wide range of extracellular materials with differing physical properties may reflect the remarkable capacity of collagen liquid crystals for reversible self-assembly into a variety of configurations which can then be locked firmly into place by intermolecular hydrogen and covalent bonding. Phase transitions in collagenous systems are certainly worth further investigation in view of the suggestion (Collings 1990) that liquid crystal transitions may be important in physiological and pathophysiological processes.

(*b*) *Advantages of the dogfish egg capsule system for studying the molecular mechanisms of collagen secretion*

The nidamental gland offers several important advantages for the study of the storage, secretion and assembly of a collagen.

A major advantage is that the rate of collagen secretion seems very high. If the assumption is made that the hydroxyproline is found only within the collagen in this system, it can be calculated from figures that we have presented elsewhere (Knight & Hunt 1974) that the helical portion of collagen accounts for approximately 20% of the dry mass of the egg capsule wall. As egg capsules are laid at a maximum rate of two every 60 h (Mellinger 1983) and each capsule has a dry mass of approximately 900 mg, the maximum rate of secretion of the helical portion of collagen is approximately 140 mg of dry protein per day. This rate of collagen secretion would appear to be a remarkable feat for two small glands together weighing less than 15 g. The cells of the D-zone of the nidamental gland appear morphologically specialized for rapid secretion possessing extensive rough endoplasmic reticulum, a very large Golgi zone, and very large numbers of secretory granules.

A second advantage is that the gland evidently stores large quantities of collagen and so has potential for the study of events occurring between transcription and the secretion of collagen. This should be facilitated by the solubility of the stored collagen and by the stability of the storage granules after dispersion in a homogenizer. The presence of large quantities of stored collagen probably results from the need to secrete egg capsules rapidly and intermittently.

A third advantage of this system is the fact that a series of morphologically distinct phases can be recognized in storage, secretion and assembly. The fact that two of these (IV and VI) are very highly ordered offers further advantage in this respect.

Finally and perhaps most importantly, there is a linear flow of secreted collagen from the apex of polarized gland cells through a series of anatomically discrete structures to the final egg capsule. Sampling at different points along the linear system will give a direct temporal sequence of changes. This has already proved useful for the study of the origins of orientation in this system (Knight & Feng 1992).

We thank Dr Brij Gupta, Rev. Dr Stephen Hunt, Dr Julian Vincent, Professor George Gray, Dr John Seeley for helpful discussion; Dr Kwok S. Kan for running polyacrylamide gels; Mr Moses Scott for catching the fish and Mr Graham Smith for storing them for us and the staff of the EM unit, Southampton General Hospital for help and advice. We gratefully acknowledge financial support from King Alfred's College and the MRC.

We apologise for overlooking the suggestion (Hukins & Woodhead-Galloway 1977, 1978) that type I collagen fibrils represent smectic A liquid crystals and dried elastoidin, smectic C.

REFERENCES

Al-Awqati, Q. 1986 Proton-translocating ATPases. *A. Rev. Cell Biol.* **2**, 179–199.

Angermann, K. & Barrach, H.J. 1979 Purification of Procollagen Type II with activated Thiol-Sepharose 4B. *Anal. Biochem.* **94**, 253–258.

Barka, T. & Anderson, P.J. 1962 Histochemical methods for acid phosphatase using hexazonium pararosanilin as coupler. *J. Histochem. Cytochem.* **10**, 741–758.

Barnard, K. & Gathercole, L.J. 1991 Short and long range order in basement membrane type IV collagen revealed by enzymic and chemical extraction. *Int. J. biol. Macromol.* **13**, 359–365.

Benedek, G.B. 1970 Theory of transparency of the eye. *Appl. Opt.* **10**, 459–473.

Berridge, M.J. & Oschman, J.L. 1972 *Transporting epithelia.* London: Academic Press.

Bouligand, Y. 1972 Twisted fibrous arrangements in biological materials and cholesteric mesophases. *Tiss. Cell* **4**, 189–217.

Bouligand, Y. 1978 Cholesteric order in biopolymers. *A.C.S. Symposium Series* **74**, 237–247.

Collings, P.J. 1990 *Liquid crystals: nature's delicate phase of matter.* New Jersey and Oxford: Princeton University Press.

Davidson, J.M. & Berg, R.A. 1981 Post-translational events in collagen synthesis. *Meth. Cell Biol.* **23**, 119–136.

Edwards, R.P. 1975 Long-spacing collagen in skin biopsies from patients with lepromatous leprosy. *Brit. J. Dermat.* **93**, 175–182.

Farber, S., Gark, A.K., Birk, D.E. & Silver, F.H. 1986 Collagen fibrillogenesis *in vitro*: evidence for pre-nucleation and nucleation steps. *Int. J. biol. Macromol.* **8**, 37–42.

Feng, D. & Knight, D.P. 1992 Secretion and stabilization of the layers of the egg capsule of the dogfish *Scyliorhinus canicula*. *Tiss. Cell* **24**, 773–790.

Forgac, M. 1989 Structure and function of vacuolar class of ATP-driven proton pumps. *Physiol. Rev.* **69**, 765–796.

Fraser, R.D.B., MacRae, T.P. & Miller, A. 1987 Molecular packing in type I collagen fibrils. *J. molec. Biol.* **193**, 115–126.

Galloway, J. 1986 Kinky variations of collagen. *Nature, Lond.* **322**, 497–498.

Gelman, R.A. & Piez, K.A. 1980 Collagen fibril formation *in vitro*; a quasi elastic light scattering study of early stages. *J. biol. Chem.* **255**, 8098–8102.

Giraud-Guille, M.M. 1989 Liquid crystalline phases of sonicated type I collagen. *Biol. Cell* **67**, 97–101.

Gray, P. 1973 *Encyclopedia of microscopy and microtechnique*. New York: Van Nostrand Reinhold.

Hukins, D.W.L. & Woodhead-Galloway, J. 1977 Collagen fibrils as examples of smectic A biological fibres. *Molec. Cryst. liqu. Cryst.* **41** (letters), 33–39.

Hukins, D.W.L. & Woodhead-Galloway, J. 1978 Liquid-crystal model for the organization of molecules in collagen fibrils. *Biochem. Soc. Trans.* **6**, 238–239.

Hunt, S. 1985 The selachian egg case collagen. In *Biology of the invertebrate and lower vertebrate collagens* (ed. A. Bairati & R. Garrone) (*NATO ASI Ser. A.* **93**), pp. 409–434.

Henry, L., Durrant, T.E. & Anderson, G. 1992 Pericapillary collagen in the human thymus: implications for the concept of the 'blood-thymus' barrier. *J. Anat.* **181**, 39–46.

Ishizeki, K., Sakakura, Y. & Nawa, T. 1987 Ultrastructural observations on the intraodontoblastic collagen fibrils of the mouse tooth germs. *Acta anat.* **128**, 164–170.

Jessen, H. 1967 The ultrastructure of odontoblasts in perfusion fixed, demineralised incisors of adult rats. *Acta odontol. scand.* **25**, 491–523.

Keene, D.R., Sakai, L.Y., Lunstrum, G.P., Morris, N.P. & Burgeson, R.E. 1987 Type VII collagen forms an extended network of anchoring fibrils. *J. Cell Biol.* **104**, 611–621.

Knight, D.P. & Hunt, S. 1974 Fibril structure of collagen in egg capsule of dogfish. *Nature, Lond.* **249**, 379–380.

Knight, D.P. & Hunt, S. 1976 Fine structure of the dogfish egg case: a unique collagenous material. *Tiss. Cell* **8**, 183–193.

Knight, D.P. & Hunt, S. 1986 A kinked molecular model for the collagen-containing fibrils in the egg case of the dogfish *Scyliorhinus caniculus*. *Tiss. Cell* **18**, 201–208.

Knight, D.P. & Feng, D. 1992 Formation of the dogfish egg capsule; a coextruded, multilayer laminate. *J. Biomimetics* **1**, 151–175.

Livolant, F. 1991 Supramolecular organization of double-stranded DNA molecules in the columnar hexagonal liquid crystalline phase. An electron microscopic analysis using freeze-fracture methods. *J. molec. Biol.* **218**, 165–181.

Livolant, F. & Leforestier, A. 1992 DNA mesophases; a structural analysis in polarizing and electron microscopy. *Molec. Cryst. Liq. Cryst.* **215**, 47–56.

Mellinger, J. 1983 Egg-case diversity among dogfish, *Scyliorhinus canicula* (L.): a study of egg laying rate and nidamental gland secretory activity. *J. Fish Biol.* **22**, 83–90.

Metten, H. 1939 Studies on the reproduction of the dogfish. *Phil. Trans. Roy. Soc. Lond.* B **230**, 217–238.

Niemalä, O., Ristell, L., Parkkinen, J. & Risteli, J. 1985 Purification and characterization of the *N*-terminal propeptide of human type III procollagen. *Biochem. J.* **232**, 145–150.

Parry, D.A.D. 1988 The molecular and fibrillar structure of collagen and its relationship to the mechanical properties of connective tissue. *Biophys. Chem.* **29**, 195–209.

Prockop, D.J., Kivirikko, K.I., Tuderman, L. & Guzman, N. 1979 The biosynthesis of collagen and its disorders. *N. Engl. J. Med.* **301**, 13–23, 77–85.

Quantock, A.J., Meek, K.M., Britain, P., Ridgway, A.E.A. & Thonar, E.J.-M.A. 1991 Alteration of the stromal architecture and depletion of keratan sulphate proteoglycans in oedematous human corneas: histological, immunochemical and X-ray diffraction evidence. *Tiss. Cell* **23**, 593–606.

Rusaouën, M., Pujol, J.P., Bocquet, J., Veillard, A. & Borel, J.P. 1976 Evidence of collagen in the egg capsule of the dogfish *Scyliorhinus canicula*. *Comp. Biochem. Physiol.* B **53**, 539–543.

Rusaouën, M. 1978 Étude ultrastructurale de zones a sécrétions protéiques de la glande nidamentaire de la rousette, a maturité. *Arch. D'anat. micr. morphol. exp.* **67**, 107–119.

Rusaouën-Innocent, M. 1990*a* Tannage quinonique de la capsule ovigére de la rousette *Scyliorhinus canicula* (Linné). *Can. J. Zool.* **68**, 2553–2563.

Rusaouën-Innocent, M. 1990*b* A radioautographic study of collagen secretion in the dogfish nidamental gland. *Tiss. Cell* **22**, 449–462.

Sawada, H., Konomi, H. & Hirosawa, K. 1990 Characterisation of the collagen in the hexagonal lattice of Descemet's membrane: its relation to type VIII collagen. *J. Cell Biol.* **110**, 219–228.

Schmid, T.M. & Linsenmayer, T.F. 1987 Type X collagen. In *Structure and function of collagen types* (ed. R. S. Mayne & R. Burgeson), pp. 223–260. New York: Academic Press.

Schneider, D.L. 1987 The proton pump ATPase of lysosomes and related organelles of the vacuolar apparatus. *Biochim. biophys. Acta* **895**, 1–10.

Stewart, M. 1986 Computer analysis of ordered microbiological objects. In *Ultrastructure techniques for microorganisms* (ed. H. C. Aldrich, & W. J. Todd), pp. 333–364. New York: Plenum.

Stewart, M. 1988 Introduction to the computer image processing of two-dimensionally ordered biological structres. *J. Electron Microsc. Tech.* **9**, 301–324.

Woessner, J.F. 1976 Measurement of the specific activities of proline and hydroxyproline in connective tissues. In *The methodology of connective tissue research* (ed. D. A. Hall), pp. 247–251. Oxford: Joynson Bruvvers.

Woodhead-Galloway, J. & Knight, D.P. 1977 The fine structure of elastoidin. *Proc. R. Soc. Lond.* B **195**, 355–364.

Woodhead-Galloway, J., Hukins, D.W.L., Knight, D.P., Machin, P.A. & Weiss, J.B. 1978 Molecular packing in elastoidin spicules. *J. molec. Biol.* **118**, 567–568.

Yurchenko, P.D. & Furthmayr, H. 1984 Self-assembly of basement membrane collagen. *Biochemistry* **23**, 1839–1850.

Received 18 December 1992; accepted 8 March 1993

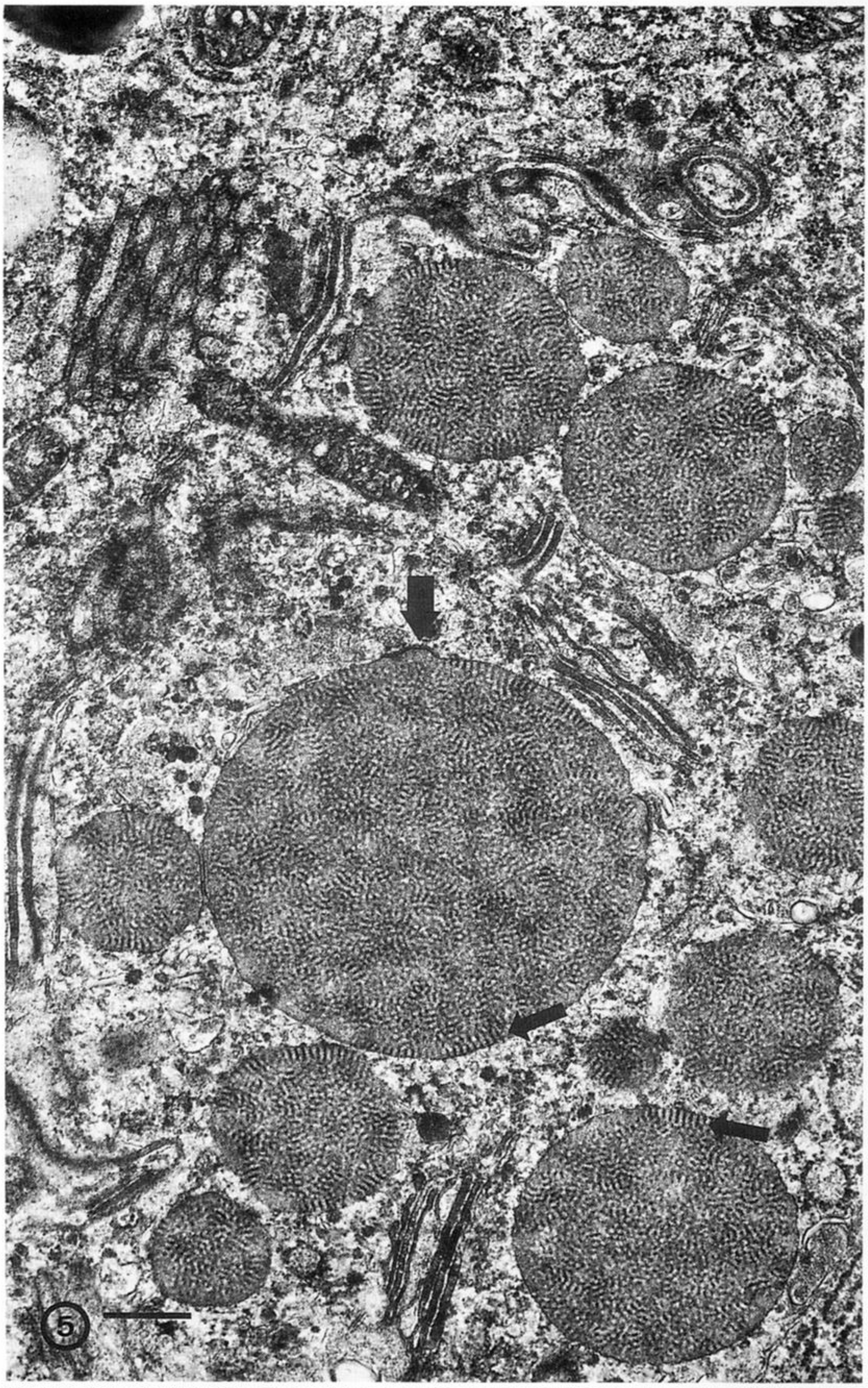

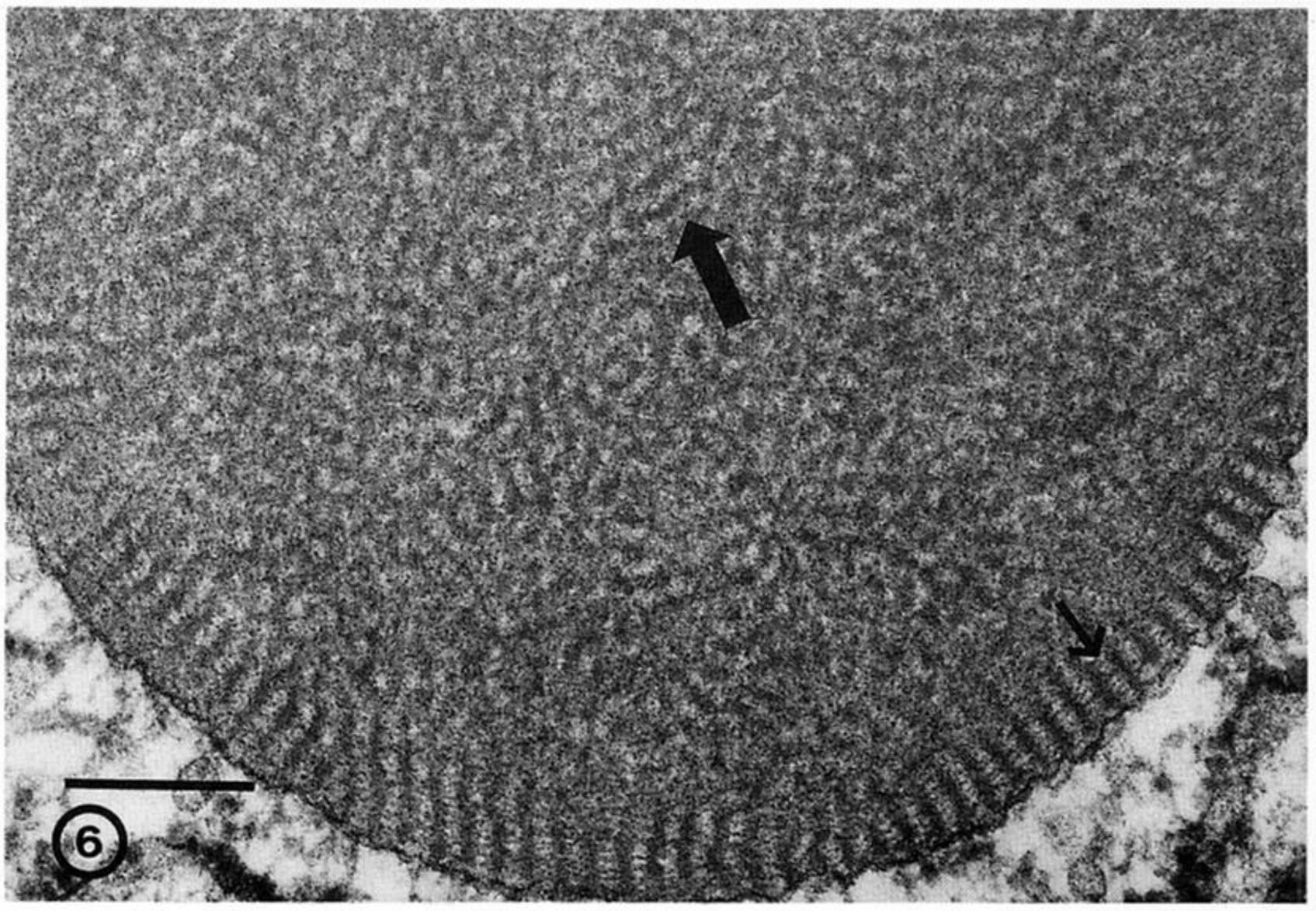

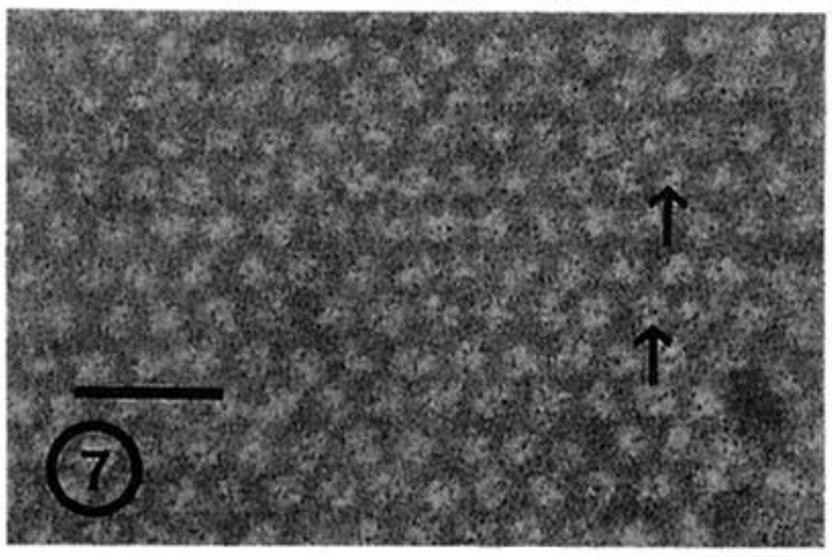

Figures 3–7. For description see opposite.

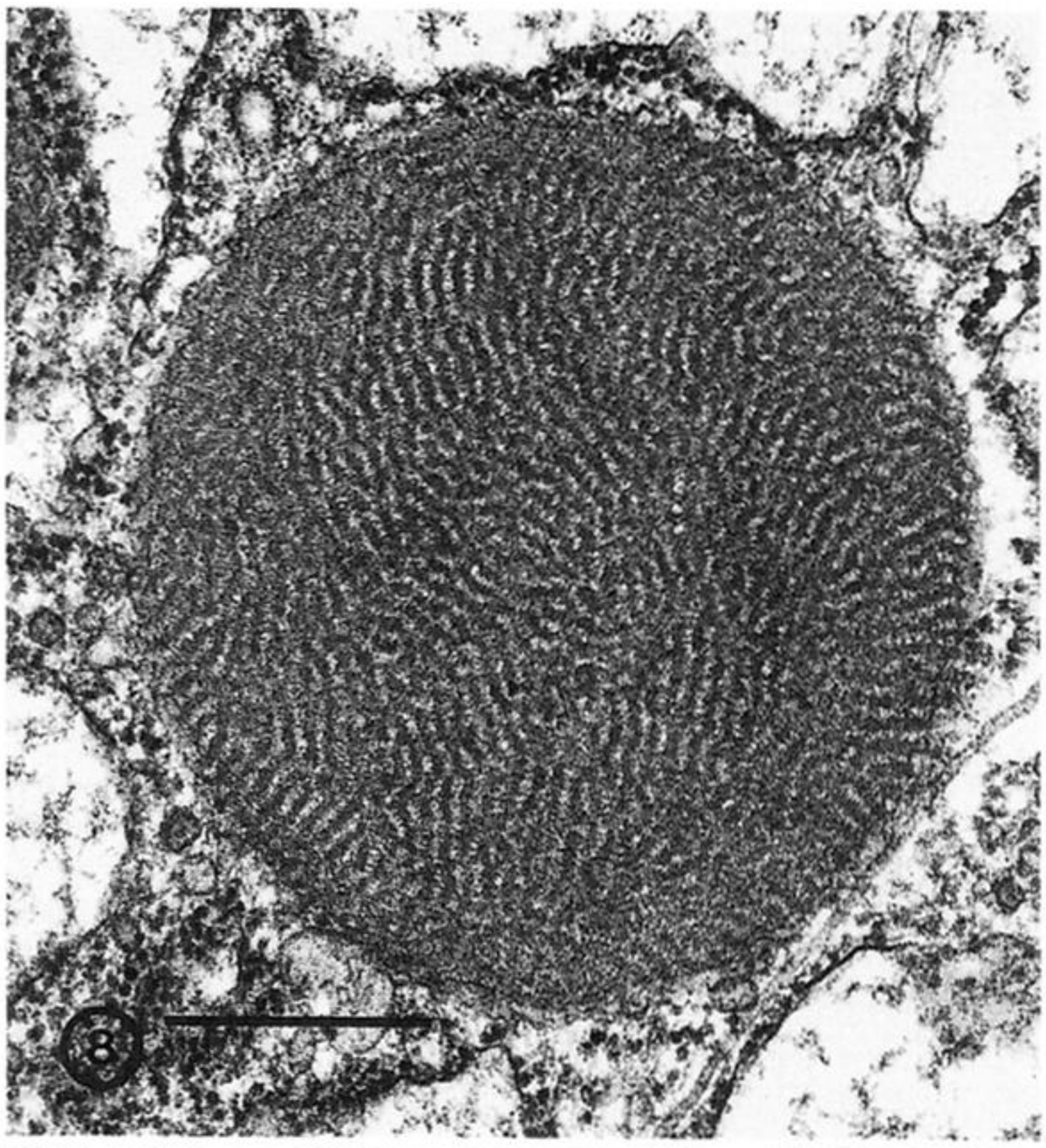

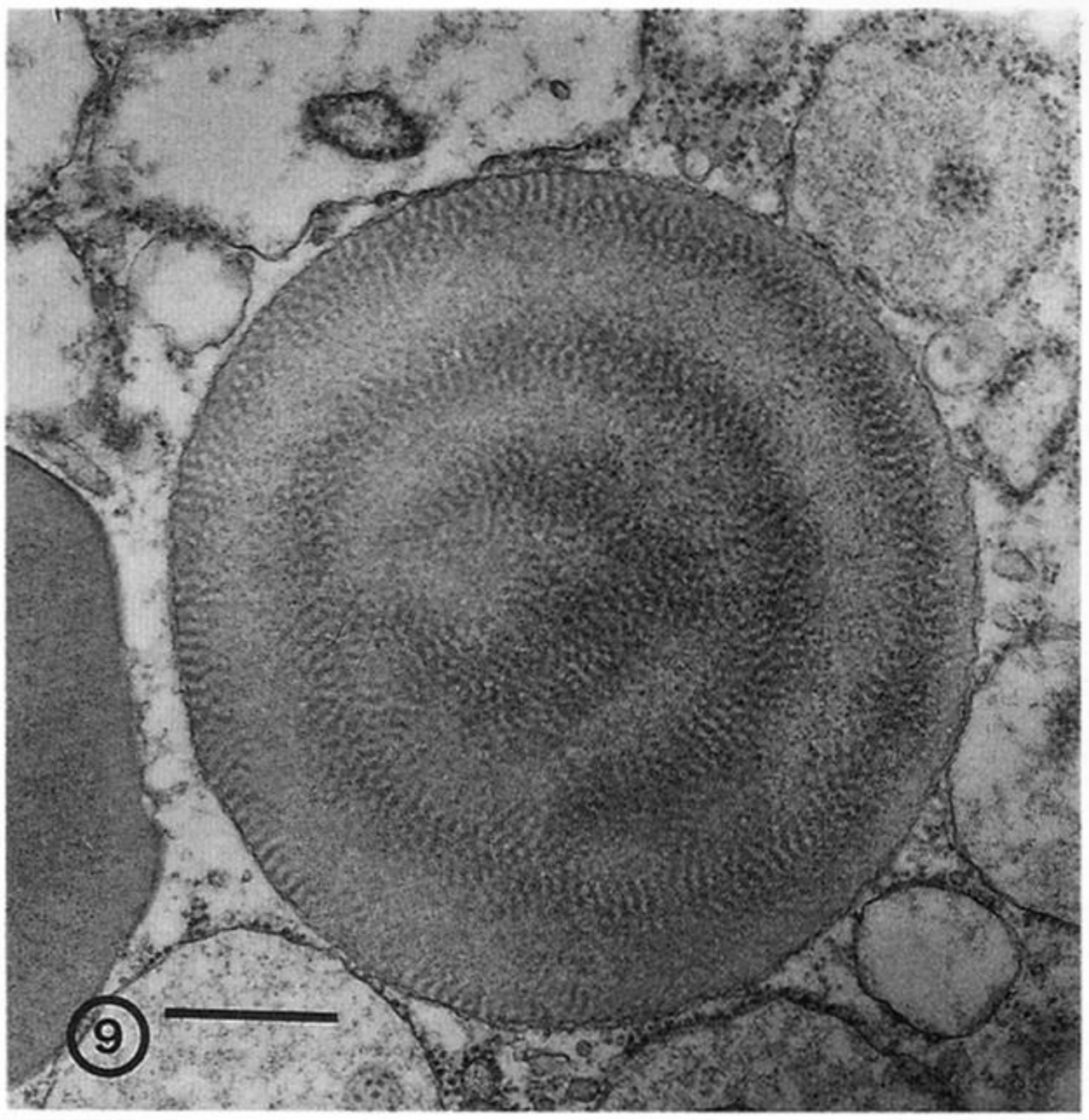

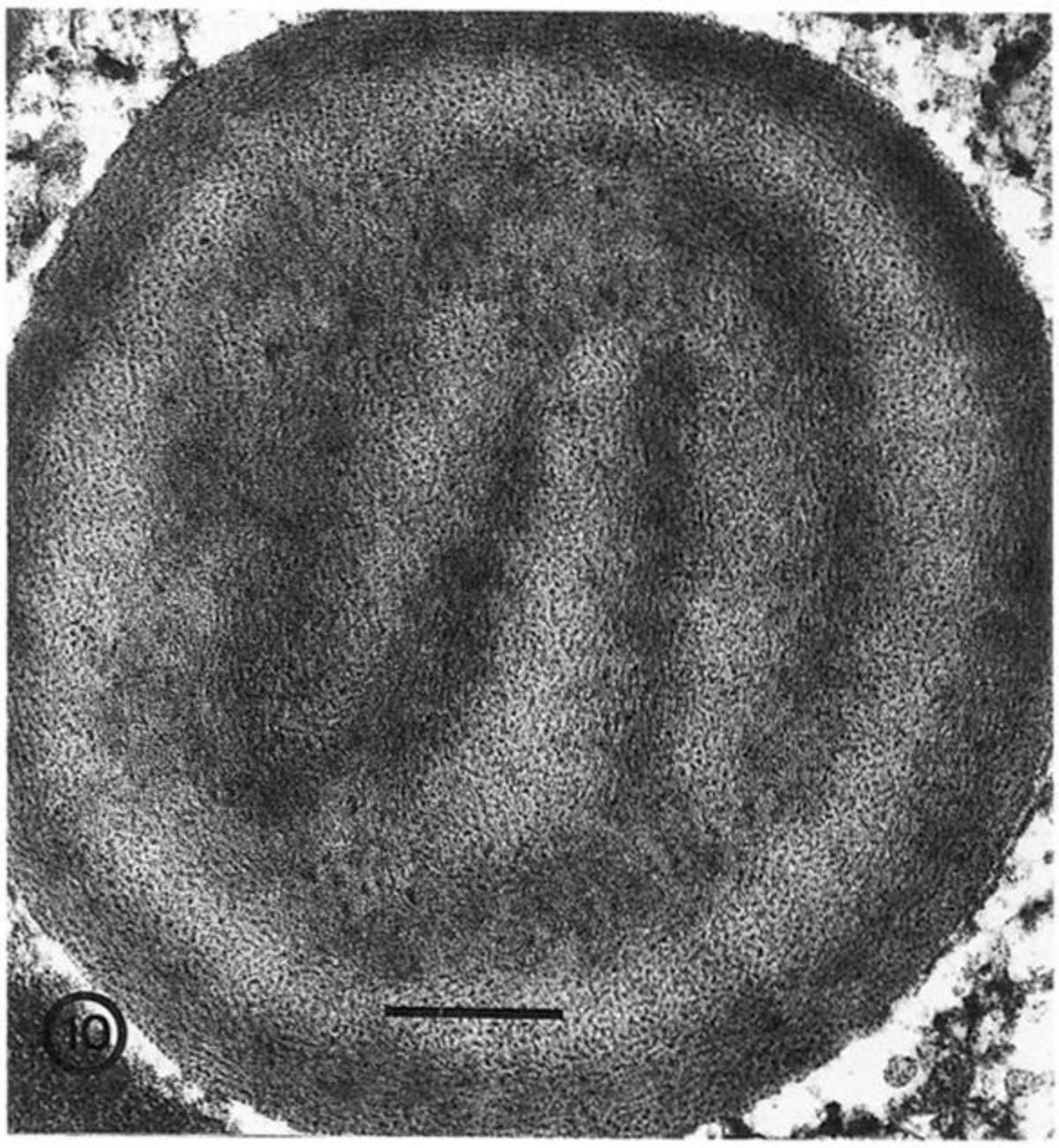

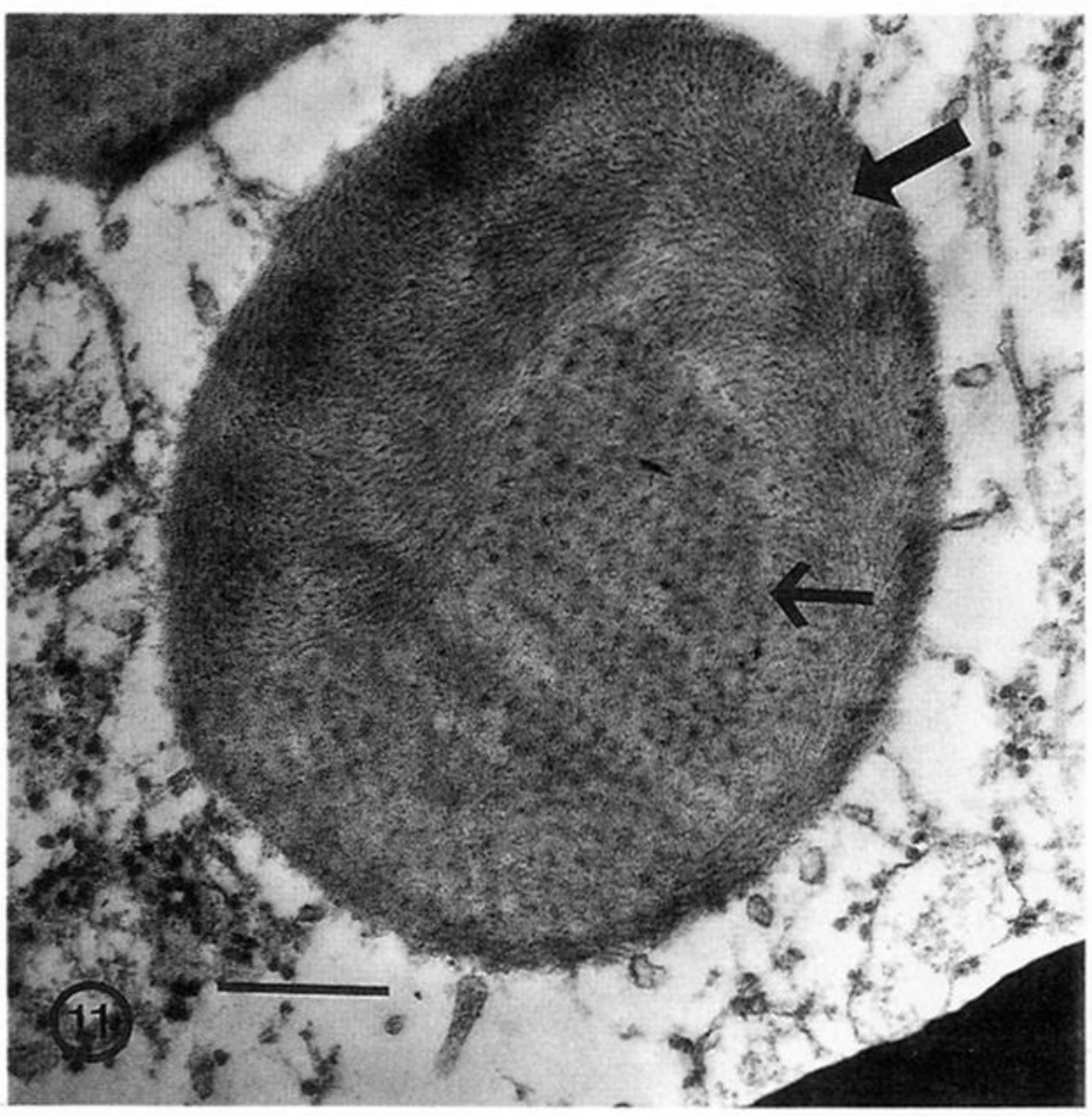

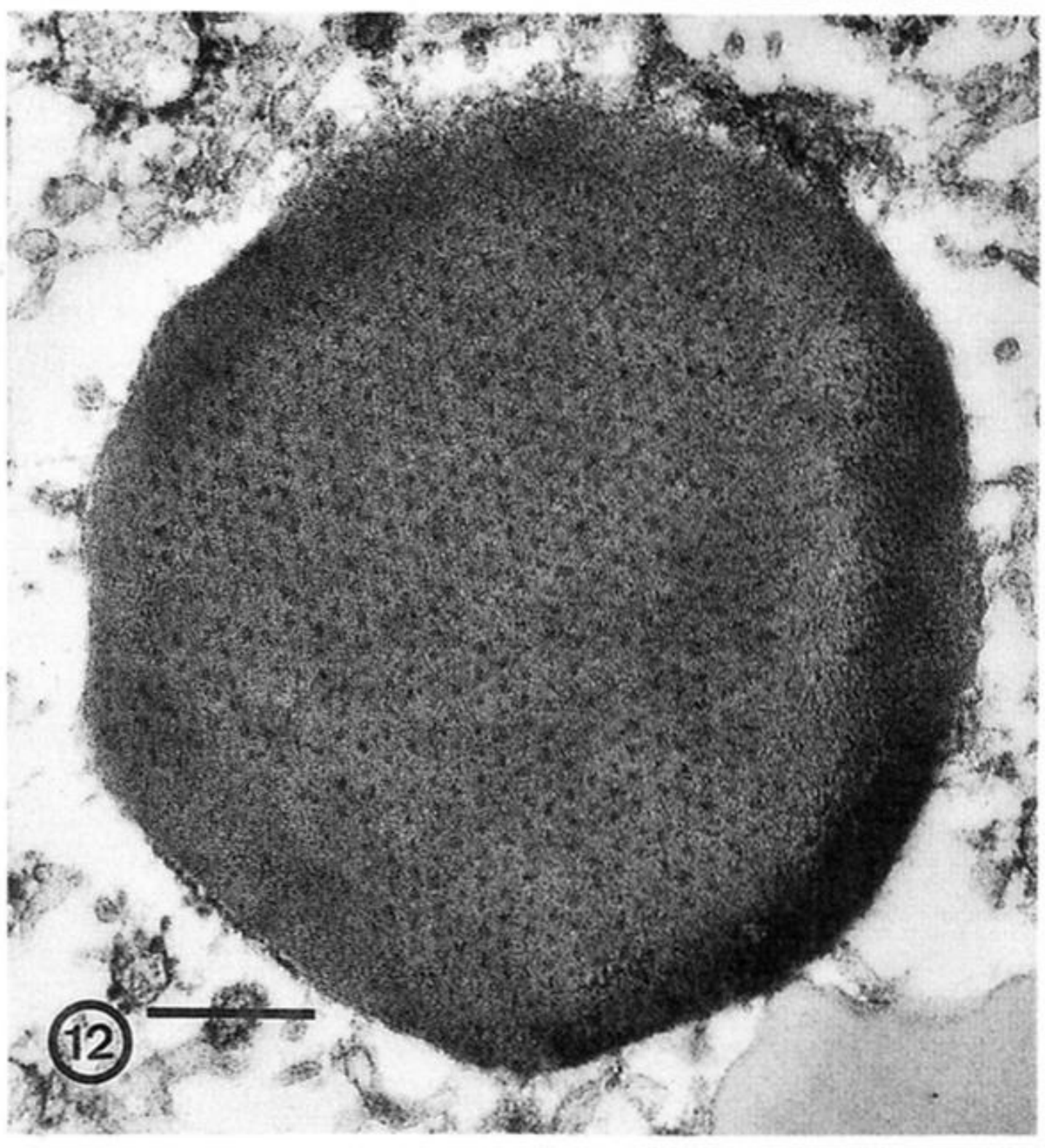

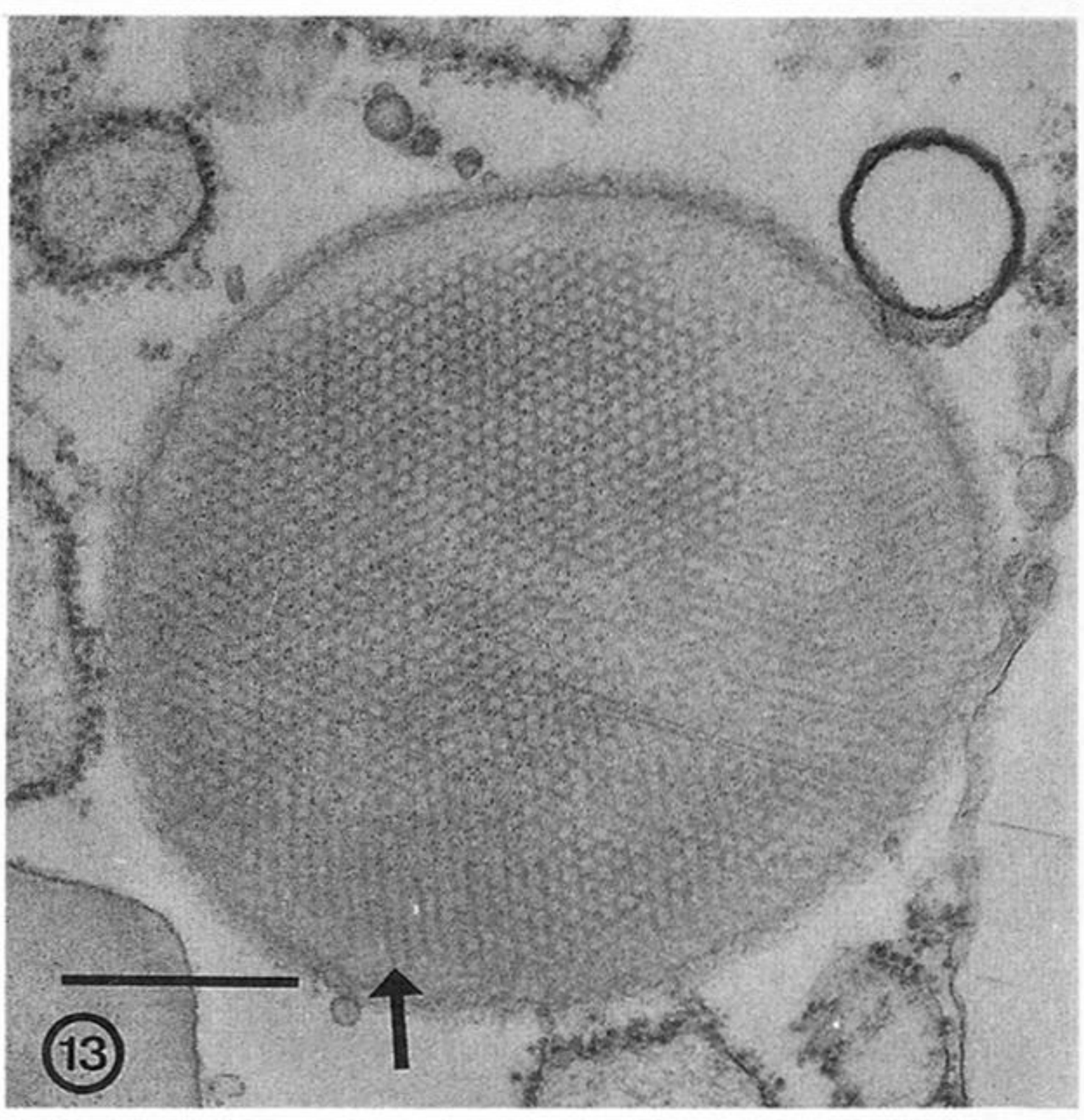

Figures 8–13. For description see opposite.

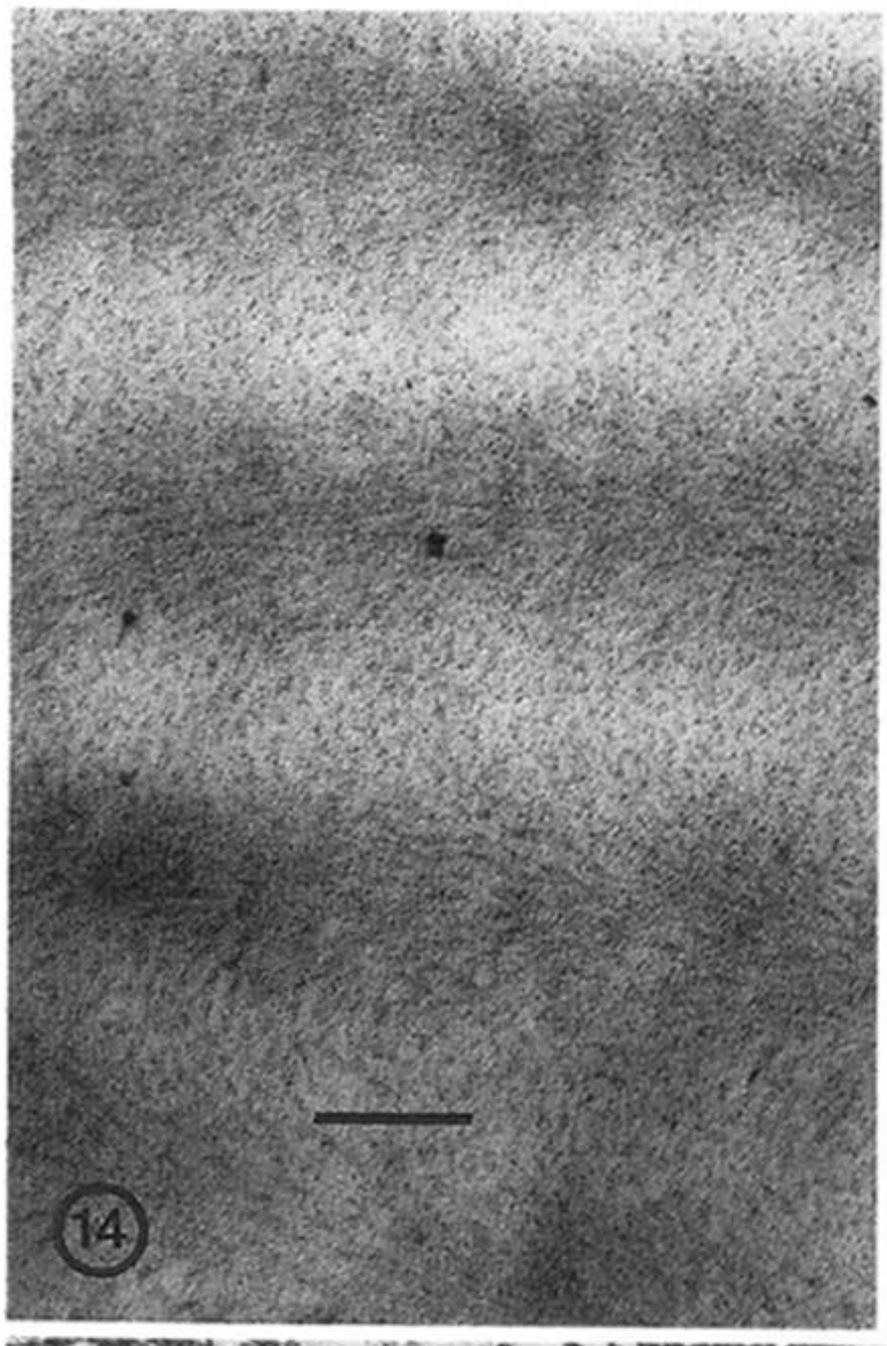

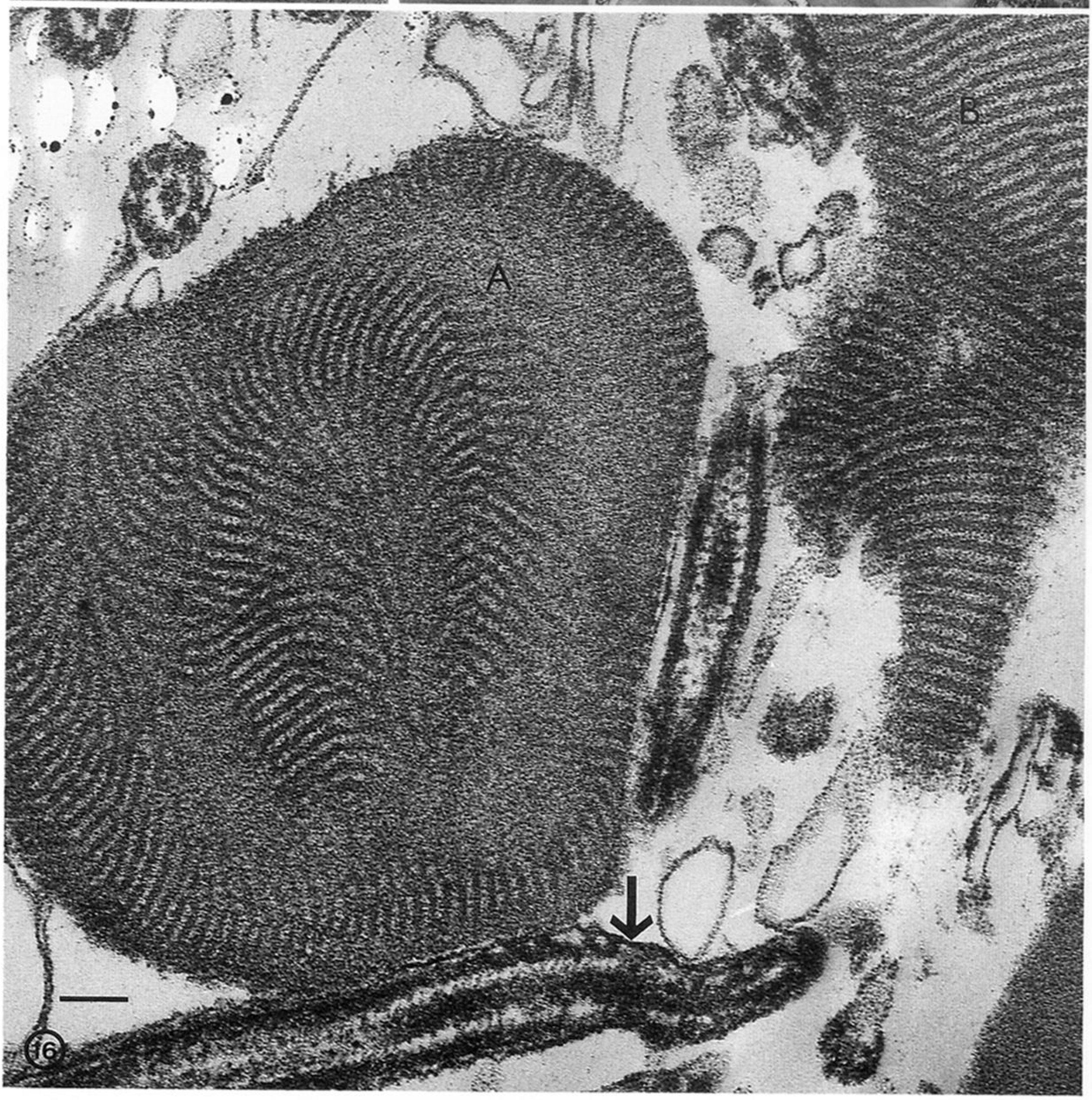

Figures 14–16. For description see opposite.

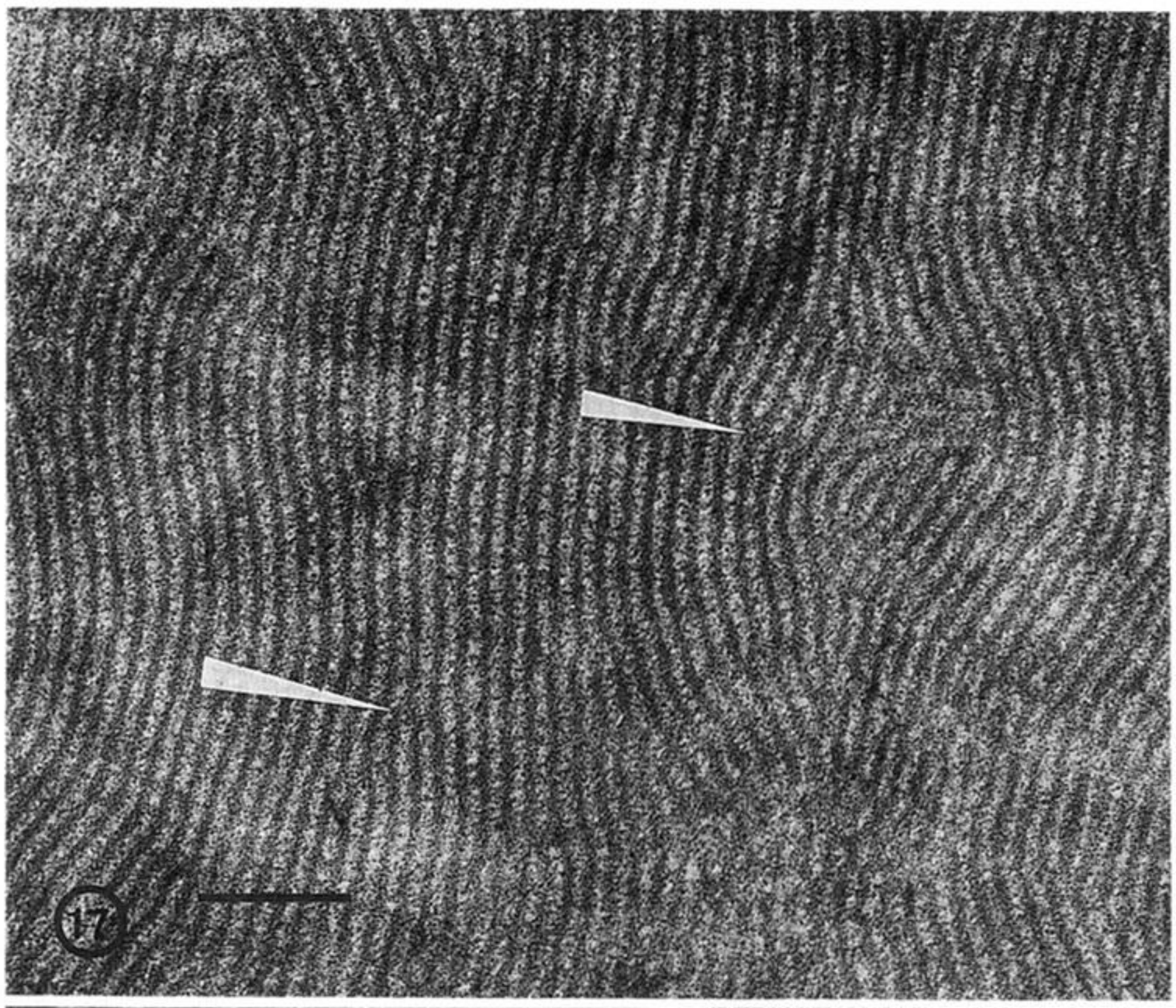

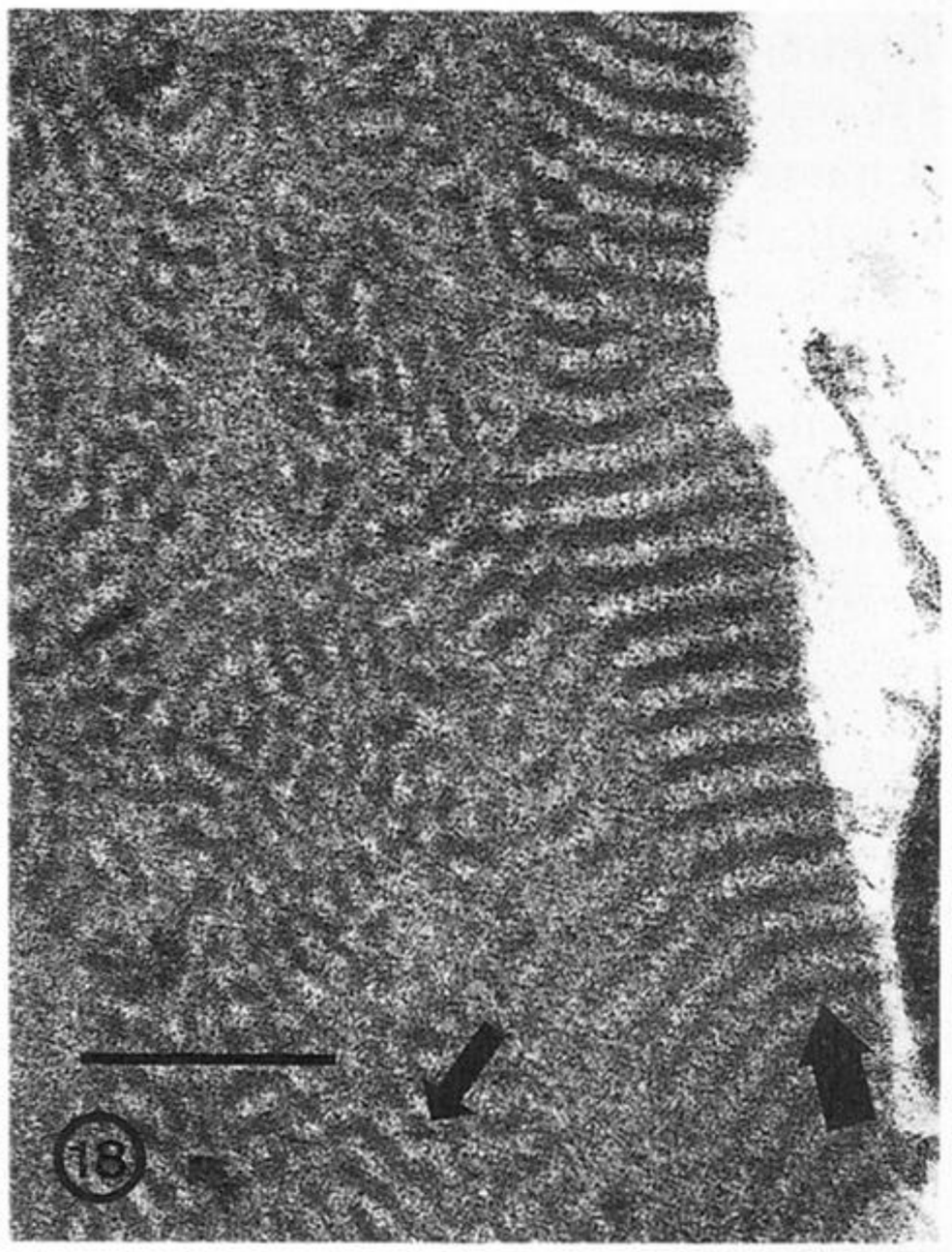

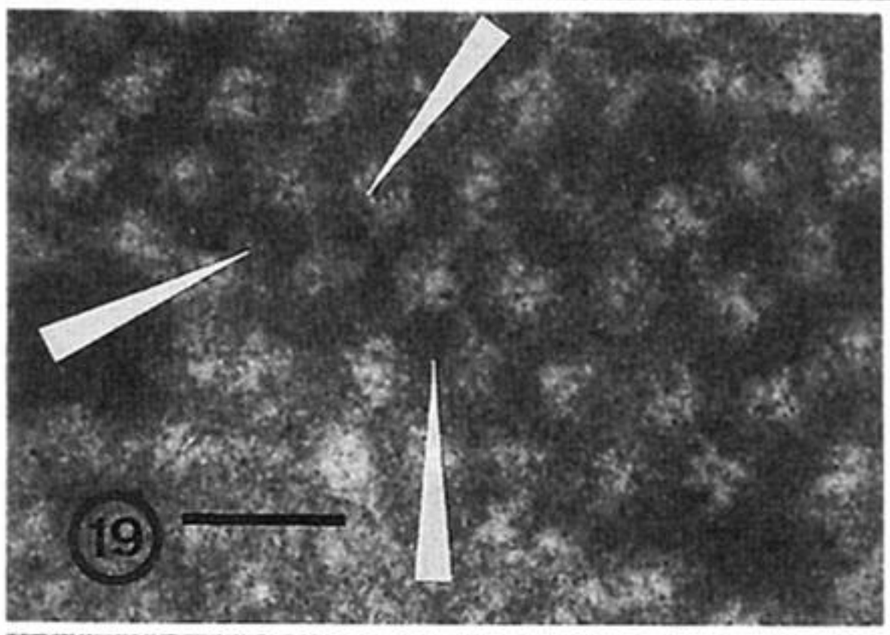

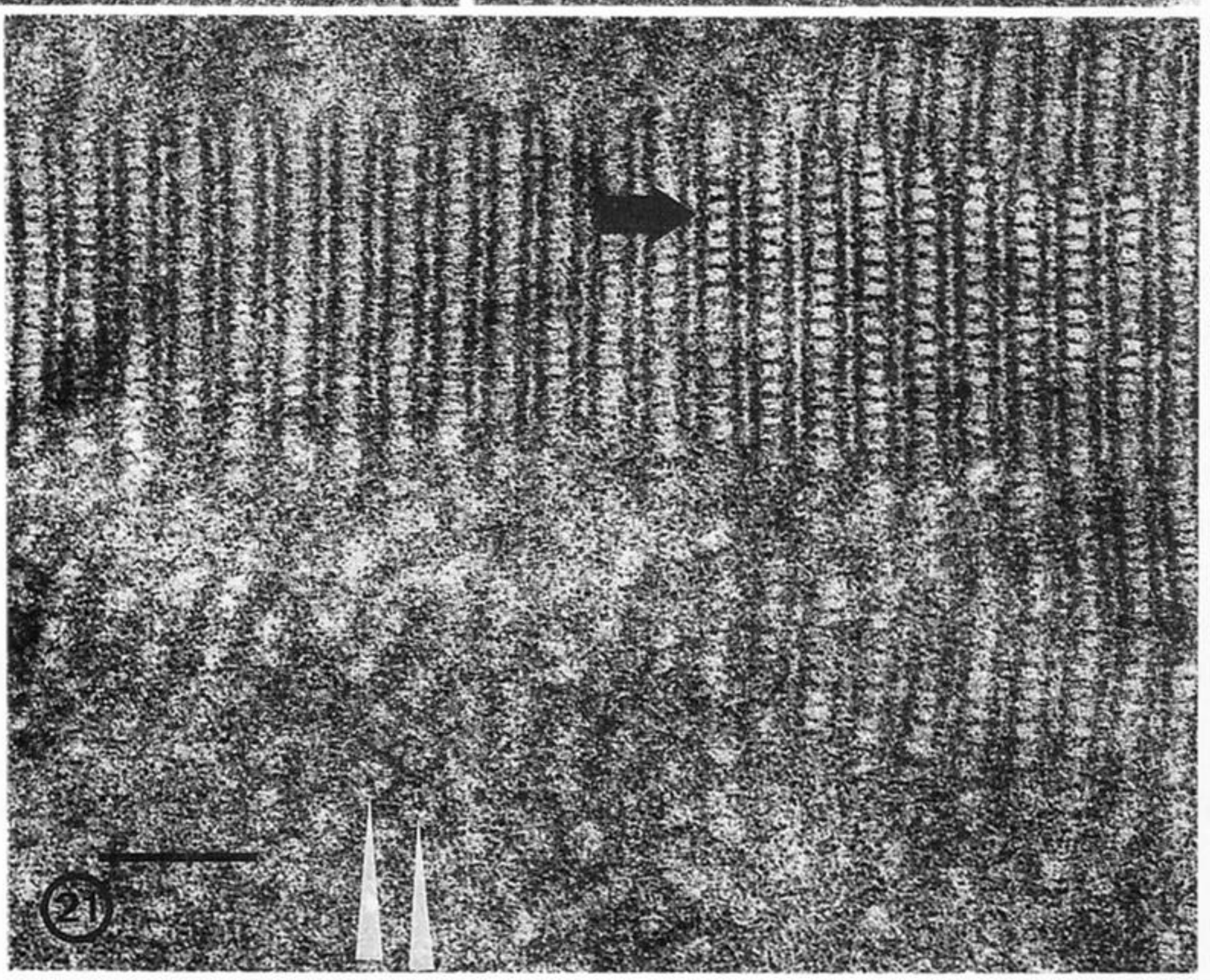

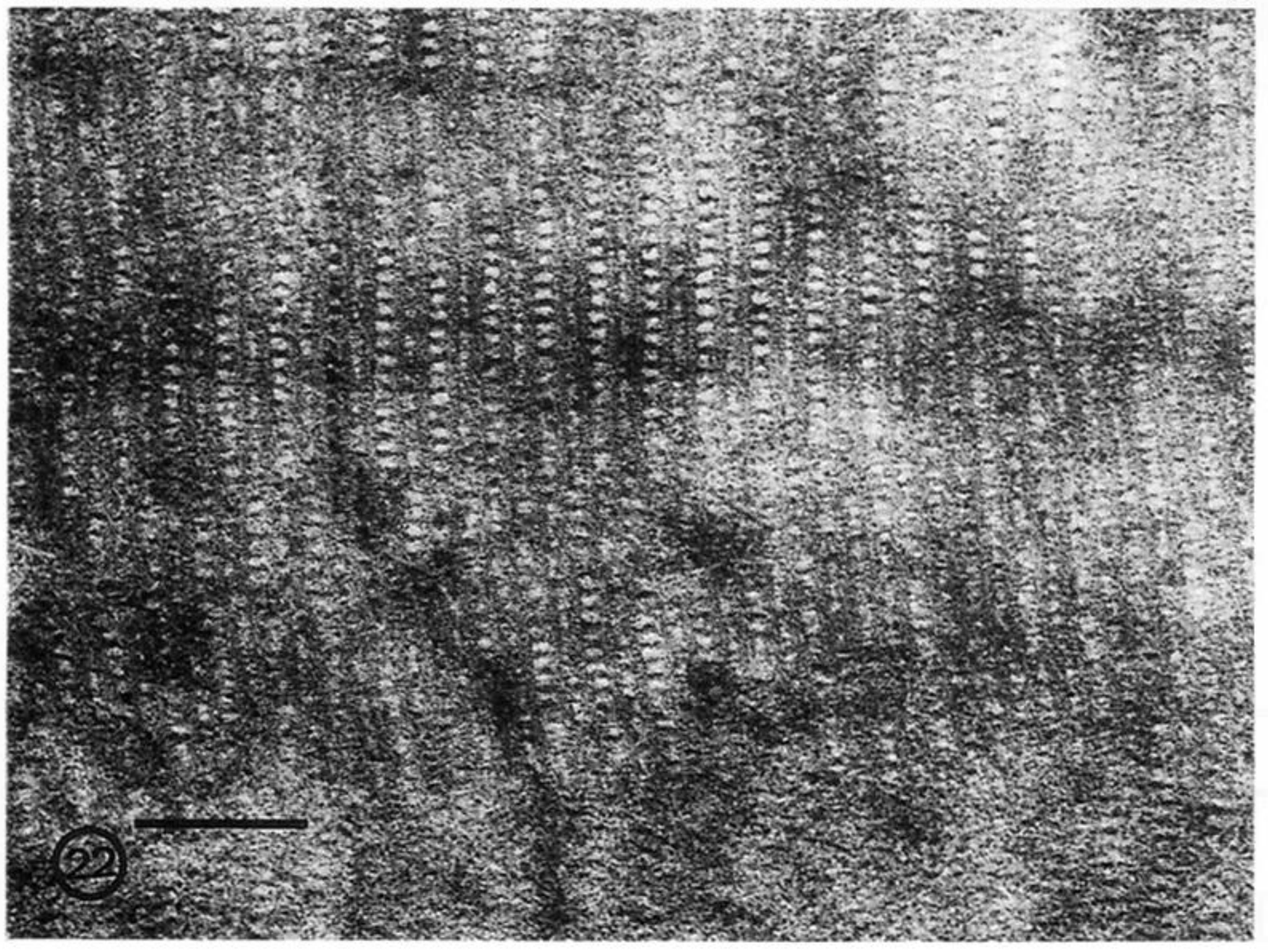

Figures 17–22. For description see opposite.

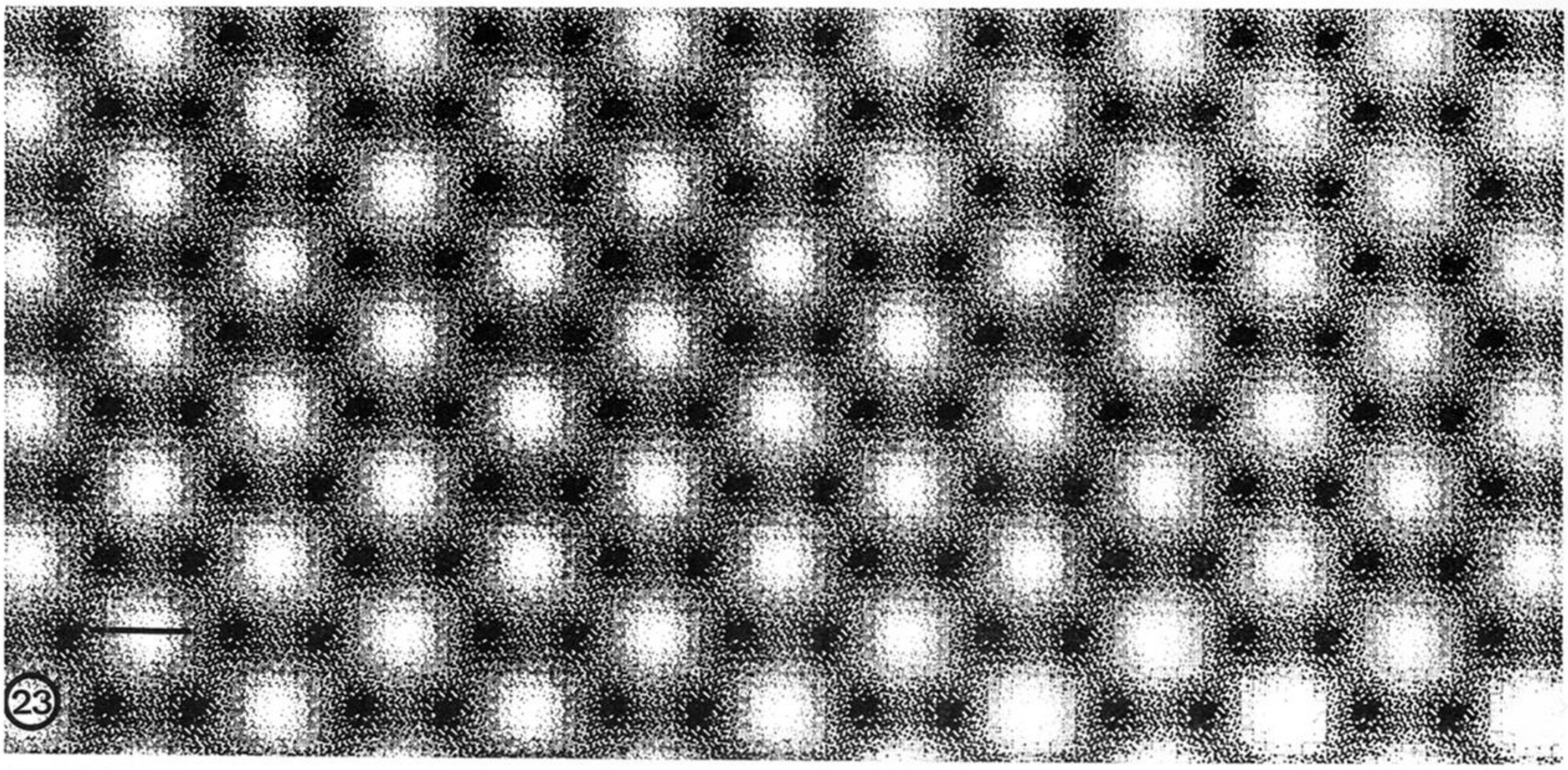

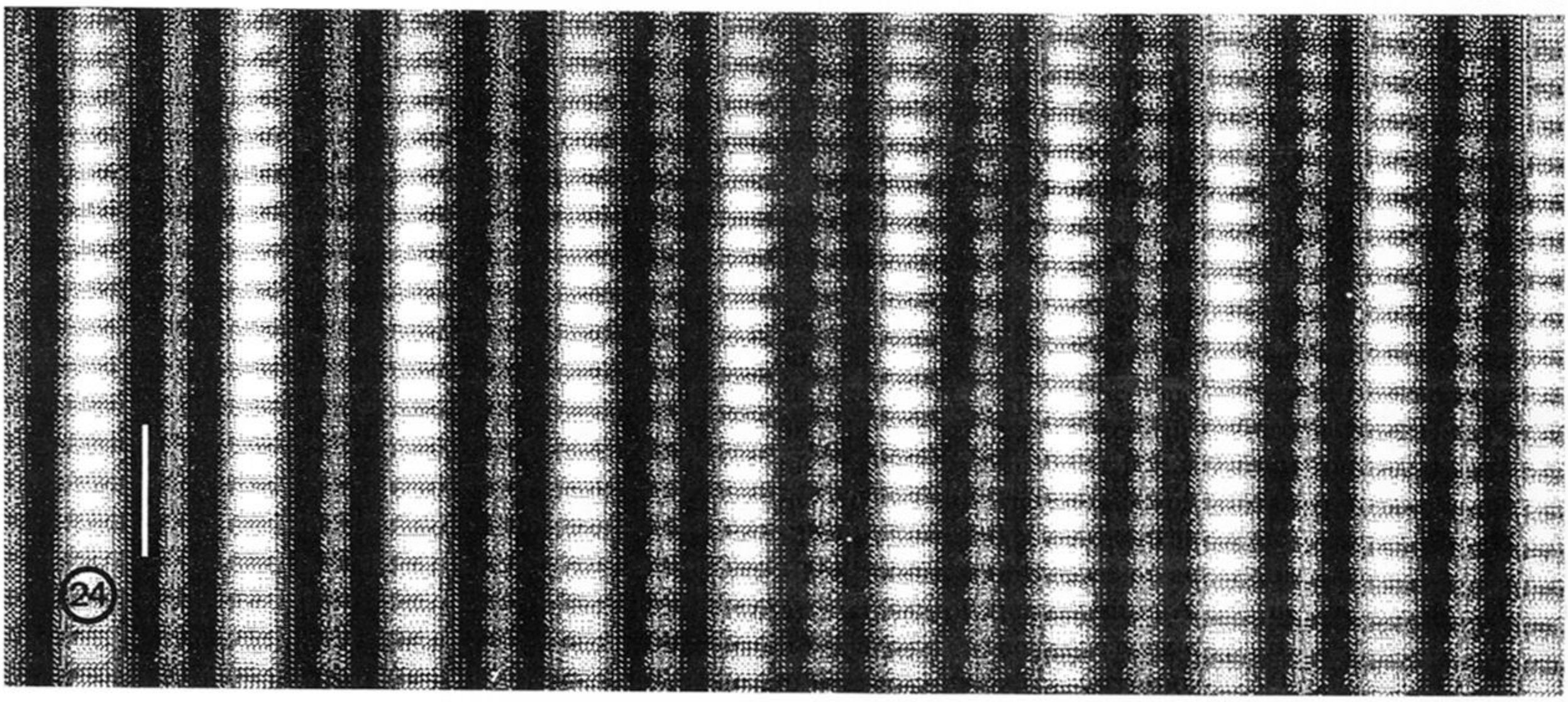

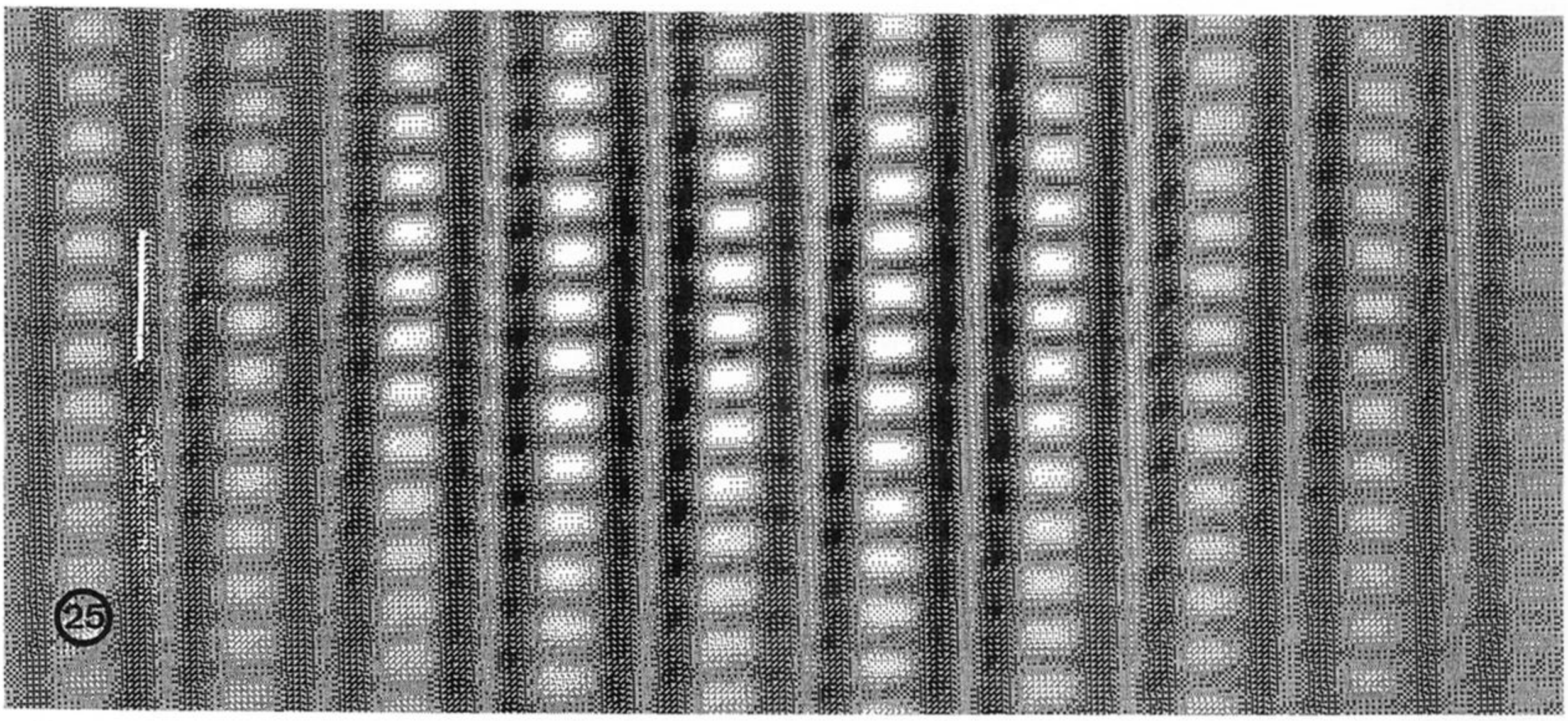

Figure 23. Reconstructed image of the hexagonal columnar phase (IV) prepared from a micrograph stained with UA and PbCit. Each hexagon contains six dense subunits. Scale bar 30 nm.

Figure 24. Reconstructed image of a longitudinally sectioned fibril (phase VI) from the white egg capsule stained with UA, PTA and PbCit. Projection 2 (Knight & Hunt 1976). Scale bar 30 nm.

Figure 25. As figure 24 but showing project 1 (Knight & Hunt 1976). Scale bar 30 nm.